MULTIVARIATE STATISTICAL CLASSIFICATION OF BEACH SANDS ALONG THE COASTAL BELT OF GHANA USING NATURAL RADIOACTIVITY DATA

This dissertation is submitted to the University of Ghana, Legon in partial fulfillment of the requirement for the award of PhD Radiation Protection

By

Henry Lawluvi, 10255977

June, 2016

DECLARATION

This dissertation is the result of research work undertaken by Henry Lawluvi in the department of Nuclear Safety and Security, University of Ghana, under the supervision of Prof. E.O. Darko and Prof. C. Schandorf.

Sign_____ _____

Henry Lawluvi Date

Sign_____ _____

Prof. E.O. Darko Date
(Principal Supervisor)

Sign_____ _____

Prof. C. Schandorf Date
(Co-Supervisor)

DEDICATION

To my late Mother

Regina Managa Senoo

(1947-2015)

ACKNOWLEDGEMENTS

I wish to express my sincere and profound gratitude to, Prof. E.O Darko, and Prof. Cyril Schandorf my supervisors for their guidance, encouragement and technical assistance. I also wish to acknowledge the support given to me by the staff of the Radiation Protection Institute and the Ghana Atomic Energy Commission for the use of their facilities. To Dr. Augustine Faanu, my Head of Department, I am grateful for your support.

I would like to show my gratitude and my love to my wife, Cathy, my sons, Yelly and Yeddy, and other members of my family for their support and love through the duration of my PhD life. One of the most important motivations to achieve my PhD has been to make you proud. Also, special thanks to all of my friends for their friendship and support.

TABLE OF CONTENTS

CHAPTER 5

RESULTS AND DISCUSSION

CHAPTER 6

CONCLUSION AND RECOMMENDATIONS

LIST OF TABLES

LIST OF FIGURES

LIST OF ABBREVIATIONS AND SYMBOLS

AEDE	Annual Effective Dose Equivalent
Hex	External Hazard Index
Hint	Internal Hazard Index
NORM	Natural Occurring Radioactive Materials
MDA	Minimum detectable activity
Raeq	Radium Equivalent
UNSCEAR	United Nations Scientific Committee on the Effects of Atomic Radiation
IAEA	International Atomic Energy Agency
ICRP	International Commission for Radiological Protection
NORM	Naturally Occurring Radioactive Materials
mSv	millisievert (10-3 Sievert)
Bq	Becquerel
Bq/g	Becquerel per gram
Bq/kg	Becquerel per kilogram
μSv	microsievert
MCA	multi-channel analyser
HPGE	High purity germanium
U	Uranium
Th	thorium
K	Potassium
SPSS	Statistical Package for Social Sciences
HCA	Hierarchical Cluster Analysis
PCA	Principal Components Analysis

ABSTRACT

The study investigated multivariate statistical data reduction strategy for environmental monitoring using radioactivity data. The activity concentrations of ^{232}Th, ^{238}U series and ^{40}K in beach sands along the coastline of Ghana have been measured using gamma spectroscopy. The mean specific activity of ^{238}U measured, ranges from 1.87 to 27.00 Bq kg^{-1}, ^{232}Th content ranges from 2.50 to 26.90 Bq kg^{-1}and ^{40}K content ranges from 47.80 to 276 Bq kg^{-1}. The values obtained in this study are comparable with published data from other works done in Ghana indicating that the study area has not been affected until now by any NORM activities that may have started in these environments. The study shows that the average Ra_{eq} value 30.93 Bq kg^{-1}, for the studied area, is lower than the internationally accepted value 370 Bq kg^{-1}. The corresponding values for the external hazard and internal hazard indices are 0.08 and 0.11 respectively. The H_{ex} and H_{in} values which are lower than the internationally accepted value of one (1.00) may not pose any significant radiological hazard to users of these sands and beaches. Hierarchical cluster analysis was used to partition the activity concentrations into non-overlapping clusters; the dendrograms revealed that ^{238}U and ^{232}Th contribute more to the Hazard Indexes than ^{40}K and the number of sampling towns can be reduced from the present 41 to 8 towns. From the analysis, it is possible to design an optimal sampling strategy, which could reduce; the number of parameters to be measured, the number of sampling stations, the number of samples collected and associated costs.

CHAPTER 1

INTRODUCTION

The quest for cost effective environmental monitoring and control, to minimize adverse health effects due to the presence of naturally occurring radioactive materials, of much concern worldwide in recent years. This chapter provides the background and explains the reason for the study, the importance, objectives and scope as previous studies have focused on different areas of the country.

1.1 Background

Exposure to ionizing radiation from natural sources is a continuous and unavoidable feature of life on earth. Radionuclides are the sources of radioactivity and they emit nuclear radiations which are a part of our environment. Alpha particles, beta particles and gamma rays are the most common forms of ionizing radiation (UNSCEAR, 2000 and Alam et. al. 2005). Radiation can arise from natural radionuclides as well as from man-made sources. Radiations have been widely applied in various fields, such as medicine, biology, industry, agriculture, and electric power generation (Singh et. al., 1999 and Alam et. al. 2005). As a result of the applications of radiation, humans can be exposed to different radioactive sources based upon their activities and surroundings (UNSCEAR, 1993 and Singh et. al., 1999). For instance, patients who are treated with medical irradiation or staff who work in the nuclear industries may receive higher radiation exposure levels than members of the general public (Radhakrishna et. al., 1993 and UNSCEAR, 1993).

The greatest contribution to mankind's exposure (both in working and public environments) are the ionising radiation arising from radionuclides in the earth's surroundings and from interaction of cosmic rays in the earth's atmosphere (De Meijer et. al., 2001). According to the United Nations Scientific Committee on the Effects of Atomic Radiation, this contribution to mankind's exposure comes from natural background radiation. The worldwide average annual effective dose per capita is 2.4 mSv. However, much higher levels of exposure are usual for inhabitants of natural high background radiation areas (HBRAs) (UNSCEAR, 2000 and. De Meijer et. al., 2001).

Exposure to naturally occurring radiation accounts for up to 85% of annual dose received by the world population, as shown in Figure 1 (Freitas et. al., 2004 and De Meijer et. al., 2001). The International Atomic Energy Agency (IAEA) reports that the exposure from natural radiation is, in most cases, of little or no concern to the public, except those working with mineral ores and naturally occurring radioactive materials (NORM) (Ramli, 1997 and Freitas et. al., 2004). However, the World Nuclear Association (WNA) states that any dose of radiation involves a possible risk to human health (Freitas et. al., 2004 and Kannan et. al., 2002), even though the level of individual exposure from naturally occurring radioactive elements is usually statistically insignificant from a health physics point of view. In order to protect the health of the general public, against the radiation risk originating from naturally occurring radiation, measurement of radioactivity in the environment is receiving a greater attention by the IAEA in recent years (Ramli, 1997 and Freitas et. al., 2004).

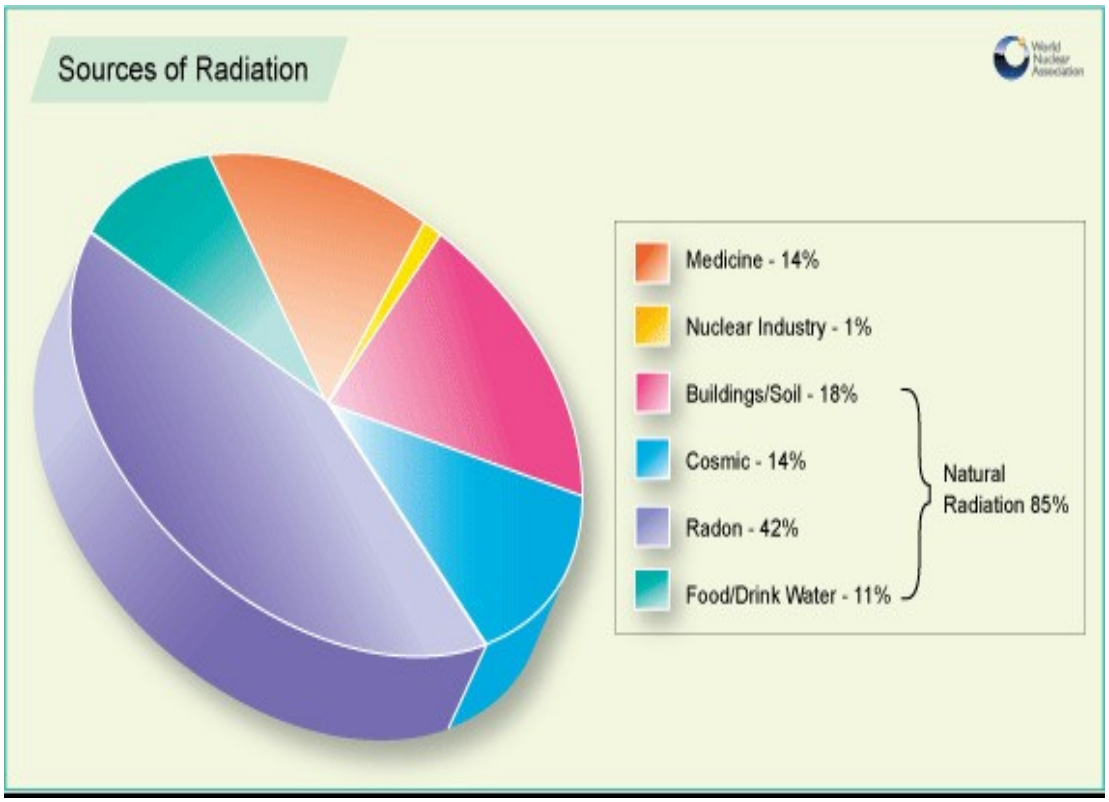

Figure 1.1: Average annual dose to the world population from various sources. (Freitas et. al., 2004 and Kannan et. al., 2002).

Naturally occurring radionuclides can be categorized as arising from two origins, namely, Terrestrial (also called primordial radionuclides) and Cosmogenic. Irradiation of the human body from external sources is mainly by gamma radiation from radionuclides in the ^{238}U and ^{232}Th series and from ^{40}K. These radionuclides are also present in the body and irradiate the various organs with alpha and beta particles, as well as gamma rays (UNSCEAR, 200).

These radionuclides are known as Naturally Occurring Radioactive Material or by the acronym 'NORM' (Freitas et. al., 2004, Paschoa, 2000). Only very long lived nuclides, with decay half-lives comparable to the age of the earth, and their decay products, contribute to this natural radiation background in significant quantities (De Meijer et. al., 2001). The majority of naturally occurring radionuclides belong to the

radionuclides in the ^{238}U and ^{232}Th series, and the single decay radionuclide, ^{40}K (Pettijohn et. al. 1987). Those radionuclides which emit either alpha or beta particles when taken into the body by ingestion or inhalation can give rise to internal exposures. Additionally, some of these nuclear species may emit gamma rays following their radioactive decay. These represent the main sources of external (whole body) exposures to humans (Radhakrishna et al., 1993 and De Meijer et. al., 2001).

Table 1.1: Ranges and averages of the concentrations of ^{40}K, ^{232}Th, and ^{238}U in typicalrocks and soils (NCRP, 1987)

Rock type	^{40}K		^{232}Th		^{238}U	
	% total K	Bq/kg	ppm	Bq/kg	ppm	Bq/kg
Igneous rocks						
Basalt (crustal ave.)	0.8	300	3–4	10–15	0.5–1	7–10
Mafic	0.3–1.1	70–400	1.6, 2.7	7, 10	0.5, 0.9	7, 10
Salic	4.5	1100–1500	16, 20	60, 80	3.9, 4.7	50, 60
Granite (crustal ave.)	>4	>l000	17	70	3	40
Sedimentary rocks						
Shale sandstones	2.7	800	12	50	3.7	40
Clean quartz	<1	<300	<2	<8	<1	<10
Dirty quartz	2a	400a	3–6a	10–25a	2–3a	40a
Arkose	2–3	600–900	2a	<8	1–2a	10–25a
Beach sands	<1	<300a	6	25	3	40
Carbonate rocks	0.3	70	2	8	2	25
All Rock (range)						
Continental crust (ave.)	2.8	850	10.7	44	2.8	36
Soil (ave.)	1.5	400	9	37	1–8	66

a indicates estimate in the absence of measured values.

Terrestrial radionuclides present in all soils at different trace levels, give rise to external exposures due to gamma radiation (De Meijer et. al., 2001). The specific levels of the radioactivity of various soils are related to the nature of the parent rock from which the soils are derived and the process of soil formation (Mange and Maurer, 1992). For example, igneous rocks, such as granite, generally exhibit higher radioactivity than sedimentary rocks (excluding some shales and phosphate rocks which have relatively high content of radionuclides) (De Meijer et. al., 2001). Tables 1.1 and 1.2 give typical natural radioactivity concentrations in common rocks, soil and other media.

Table 1.2: Natural concentration of some terrestrial radionuclides in various media (Van der Stritch 2001).

Medium	Activity Concentration in Bq/kg			
	^{40}K	^{226}Ra	^{232}Th	^{238}U
Soils	400	40	25	25
Granite	1000	100	80	60
Coal	<40	<20	<20	-
Fertilizers	<4000	<400	<20	-
Ground water	<1	<1	<1	<1
Seawater	10	<1	<1	0.04
Drinking-water	0.2	<1	-	0.004
Milk	47	0.003	-	0
Foodstuffs	40-300	0.01-100	-	-
Man	~60	0.03	-	0.1

1.2 Problem Statement

All living organisms of the planet are exposed to natural radiation, which is mainly due to the activity concentration of primordial radionuclides ^{232}Th, ^{238}U and their decay product, and ^{40}K which are present in the earth's crust (UNSCEAR, 2000). According to Ramli (1997), one of the major interests in studies of natural background radiation is the need to establish reference levels, especially in areas where the risk of radioactive material being released to the environment is high. There is, also a worldwide interest in identifying new areas with high natural radiation. Several authors have studied the levels of natural background radiation by in situ measurements or by analysis of radionuclides concentrations in soil or sand samples. However, with increasing demands for data of defensible quality, environmental protection agencies are faced with a substantial societal expenditure constrains. The United States Environmental Protection Agency (EPA) estimates that about $5 billion is spent annually by the EPA and the regulated community collecting data for research, regulatory decision making and regulatory compliance (USEPA, 1994).

This situation could pose a big financial challenge to the Nuclear Regulatory Authority of Ghana as well as other environmental safety conscious organisations, as the country makes frantic efforts in promoting its environment to the outside world.

This work is to develop an optimal future sampling strategy which could reduce number of sampling sites and associated sampling (and analysis) costs.

1.3 Objectives of the Research

Main Objective of this study is to develop a cost effective Coastline sampling strategy for Beach Sands through the application of a Multivariate Statistical Technique to natural radioactivity data.

The specific objectives of this research are to:

i. evaluate the activity concentration of ^{40}K, ^{238}U, and ^{232}Th in beach sands, and estimate Absorbed Dose Rate;
ii. assess the radiological health impact, from exposure to radionuclides in beach sands, on the public using Hazard Indices (H_{ex} and H_{in}), Effective Dose, Radium Equivalent (Ra_{eq}) and ELCR;
iii. establish a relationship between radionuclide activities and radiological parameters using multivariate Statistical techniques;
iv. identify and classify beach sands into spatial groups on the basis of similarities or differences among their natural radioactivity concentrations using Cluster Analysis.

1.4 Scope of Research

This study measured and related the activity concentrations of ^{40}K, ^{238}U (^{226}Ra) and ^{232}Th, in beach sands from Landing and Tourist beaches along the coastal belt of Ghana. The activity concentration data was used to classify the beach sands using multivariate statistical techniques.

1.5 Relevance of Work

Ghana's coastline covers a distance of 550 km stretching from Aflao in the East to Half-Assini in the West. Due to the vast coastline, monitoring Natural Radionuclides in beach sands is very tedious, time consuming and have huge financial implications. There is the need to classify or group the beach sands in other to make monitoring less tedious and cost effective. This called for the development of a sampling strategy along the coast using a statistical tool to facilitate NORM monitoring.

In this study, Multivariate Statistics (Hierarchical Cluster Analysis) was used to classify the beach sands for NORM monitoring

The outcome of this work will assist in proposing an optimal future sampling strategy which could reduce number of sampling sites and associated sampling and analysis costs.

1.6 Arrangements of Chapters

Chapter 1 provides the background and explains the reason for the study, the importance, objectives and scope as previous studies have focused on different areas in the country. In Chapter 2, Natural Occurring Radioactive Materials (NORMs) in the environment and their identification and quantification using HPGe based gamma-ray spectroscopy are reviewed. Principles of multivariate statistical techniques as well as their utility in multivariate data analysis are also discussed. Chapter 3 gives a description of the Study Area. Chapter 4 discusses the materials and methods used to carry out the research work. Chapter 5 outlines the results and associated discussions. Chapter 6 summarizes the major conclusions of this study and makes recommendations to relevant stakeholders.

CHAPTER 2

LITERATURE REVIEW

In this chapter Natural Occurring Radioactive Materials (NORMs) in the environment and their identification and quantification using HPGe based gamma-ray spectroscopy are reviewed. Principles of multivariate statistical techniques as well as their utility in multivariate data analysis are also discussed.

2.1 Naturally Occurring Radioactive Materials in the Environment

Naturally occurring radionuclides of terrestrial origin (also called primordial radionuclides) are present in various degrees in all media in the environment, including beach sand. Only those radionuclides with half-lives comparable to the age of the earth, and their decay products, exist in insignificant quantities in these materials. Irradiation of the human body from external sources is mainly by gamma radiation from radionuclides in the ^{238}U and ^{232}Th series and from ^{40}K. These radionuclides are also present in the body and irradiate the various organs with alpha and beta particles, as well as gamma rays (UNSCEAR, 2000).

There have been many studies concerning naturally occurring radioactive materials in soil media, which provide information on the nature and levels of background radiation as well as the change in radioactivity levels in that particular area. Most of these studies show that most soils contain ^{40}K and nuclides of the uranium and thorium series, with a range of their concentrations that varies broadly. For example, the investigation of the concentrations and distribution of radioactive nuclides in river sediments and coastal soils in Chittagong, Bangladesh was carried out by Chowdhurry, Alam, and Hazari (Chowdhury et. al., 1999). The results of the

activity concentrations of ^{238}U, ^{232}Th, and ^{40}K are higher than the average world values which are 35, 30, 400 $Bq.kg^{-1}$ (UNSCEAR, 2000), respectively. In 2004, Matiullah, Shakeel, Shafi, and Faheem reported the mean activity of ^{226}Ra, ^{232}Th, ^{40}K, and ^{137}Cs in soil samples of Bahawalpur, Pakistan being 32.9, and 53.6, 647.4 and 1.5 $Bq.kg^{-1}$ (Matiullah et. al., 2004). In the same year, the activity concentration levels arising from radionuclides ^{238}U, ^{232}Th,and ^{40}K in surface soils in Cyprus were carried out by Tzortzis, Svoukis, and Tsertos ranging between 0.01-39.3, 0.01-39.8 and 0.04-565.8 $Bq.kg^{-1}$, respectively (Tzotzis et. al., 2004). Soil and sediments were used for measuring the natural radioactivity levels of Firtina Valley in Turkey by the team of Karadeniz Technical University, University of Rize, and Cekmece Nuclear Research and Training. The average concentrations of ^{238}U, ^{232}Th, ^{40}K, and ^{137}Cs in the area surveyed in that study were found to be 50, 42, 643, and 85 $Bq.kg^{-1}$ in soil samples, and 39, 38, 573 and 6 $Bq.kg^{-1}$ in sediment samples (Kurnaz et. al., 2007). Activity concentrations were measured from sediment samples collected along the Upper Egypt Nile River region in 2007 by El-Gamal, Nasr, and El-Taher. The measurement showed ranges of ^{238}U, ^{232}Th, and ^{40}K concentration of 3.83-34.94, 2.88-30.10 and 112.31-312.98 $Bq.kg^{-1}$ (El-Gamal et. al., 2007). Al- Hamarneh and Awadallah determined the radioactivity levels in various geological formations of soils in the northern Highlands of Jordan in 2009. The average radioactivity concentrations were 42.5, 49.9, 26.7, and 291.1 $Bq.kg^{-1}$of ^{226}Ra, ^{238}U, ^{232}Th, and ^{40}K, respectively (Al-Hamarneh and Awadallah, 2009). Some studies show the remaining artificial radioactive nuclide ^{137}Cs can be detected in some areas (Chowdhury et. al., 1999, Tzotzis et. al., 2004 and Kurnaz et. al., 2007).

Knowledge of the concentrations and distributions of the radionuclides in soil

materials are of interest since they provide useful information on the monitoring of environmental contamination by radioactive materials in the natural environment. Enhanced levels of radioactivity in particular areas can arise due to the discharges of radioactive nuclides following human intervention (Bikit et. al., 2006, Bolca, 2007 and Carvalho, 2007). Thus, it is necessary to consider all of the significant sources of radioactive nuclides present in the environment. Human activities, such as adding fertilizer, importing top soil and the like can alter the surface radioactivity (NCRP, 1975). Agricultural history is important in the concentration of nuclides in soils. The use of fertilizers in various agricultural situations has affected radionuclide concentrations to a large extent. Also, fertilizers may affect the chemical form of natural radionuclides in soils and, thus their physical transport and biological uptake (Klement, 1982).

According to Khater, the application of phosphate fertilizers has substantially increased in the world (Khater and Al-Sewaidan, 2008). Furthermore, several authors have stated that the cultivated lands may be contaminated with trace metals and some naturally occurring radioactive materials (NORM) by using phosphate fertilizers in the agriculture activities (Khater and Al-Sewaidan, 2008, Ahmed and El-Arabi, 2005, Jibiri et al.2007 and Saueia and Mazzilli, 2006).

A determination of the concentration and the distribution of soil radioactivity is essential in establishing reference data, allowing the observation of possible future changes due to future radiological contamination (Ramli, 1997).

In 1997, Sohrabi carried out a review study on areas with elevated levels of NORMs (Lilley, 2001). This study concluded that elevations of NORM in different regions are mostly due to either "geological structure and geochemical movements

of the radioactive materials in the soil, such as Morro de Ferro and Meaipe in Brazil" (Carvalho et. al., 2007), Kerala coast in India (Khater and Al-Sewaidan, 2008, Jibiri et. al., 2007) and Yangjiang in China, where the origins of the elevated NORMs are due to monazite sands which are rich in thorium (Jibiri et. al., 2007). Most of these areas are considered as medium-level natural radiation areas (MLNRA), with an average dose rate to the public of 6.4 mGy/y in Meaipe (Saueia and Mazzilli, 2006). However, Kerala in India is classified as high level natural radiation area (HLNRA) with an average dose rate exceeding 10 mGy/y (Saueia and Mazzilli, 2006). In some areas in US such as Denver, CO, and Reading Prong, PA the radiation level was 10 times more than the usual concentration, being rich in uranium series radionuclides in the soil (Ramli, 1997).

Other origins that may elevate the levels of natural radioactivity include phosphate deposits. This type of NORM occurs for instance in Florida, USA (Bolca et. al., 2007). The uraniferous granite and alum shale distribution can also increase radiation exposure, not only within dwellings (as the case in Sweden) but also in the outdoor area (Bolca et. al. 2007). Using construction materials rich in ^{226}Ra content (such as tailing from uranium mining) in areas for example Joachimstal in Czech Republic and Schlema, Schneeberg, and Saxony in Germany have been the main reason of indoor exposure due to very high levels of ^{222}Rn (Wikimedia Commons, 2009). Saxony has been classified as a very high level natural radiation area (Saueia and Mazzilli 2006). Water rich in ^{226}Ra and ^{222}Rn from hot springs which flow in Badgastein in Austria (UNESCO, 2003), and Mahallat and Ramsar in Iran (L'Annunziata, 2007), has been found to cause elevation of exposure, as high as 55 mSv/y for people working in the spa centres using the hot spring water for therapeutic purposes (Bolca et. al. 2007).

Several authors have studied the radionuclide concentrations in beach sand in Kerala and Tamil Nadu coastal regions of India (UNSCEAR, 1982) and in South-western Australia (UNSCEAR, 1993). Also in India, they analysed the distribution of natural and anthropogenic radionuclides in beach sand and soil from Kalpakkam (Radhakrishna et. al., 1993) area using gamma-ray spectrometry. Freitas and Alencar (Freitas and Alencar, 2004) studied the process of dispersion and the activity concentration of ^{232}Th and ^{238}U series and ^{40}K radionuclides in two island beaches in south-eastern Brazil. They found that the absorbed dose rate in air, observed at 1 m above the ground, ranged from 54 to 228 nGy h^{-1} at Preta beach and from 39 to 110 nGy h^{-1} at Dois Rios beach.

2.1.1 Decay of Naturally Occurring Radionuclides

Naturally occurring radionuclides can be grouped into two categories: single decays and three main radioactive decay series. Decay chains from terrestrial radionuclides have been present since the birth of the earth, headed by the radionuclides ^{235}U (half-life 7.04×10^{8} years), ^{238}U (half-life 4.47×10^{9} years), and ^{232}Th (half-life 1.41×10^{10} years) (UNSCEAR, 1993). Naturally occurring uranium consists of three separate radioisotopes with present day isotopic abundances of 99.3% for ^{238}U and about 0.7% for ^{235}U, plus a small amount of ^{234}U (5×10^{-3}%) (Cember and Johnson, 2009). The ^{238}U and ^{234}U isotopes are part of the same series (the “uranium” series), while ^{235}U is the first radionuclide of another family called the actinium series. Uranium has been found in all rocks and soils with an average concentration in the range of 1-3 parts per million (ppm) by weight, which corresponds to a specific activity of ~74 mBq.g^{-1} soil (Cember and Johnson, 2009). The relationship between uranium and P_2O_5 content of fertilizer has been

investigated in various studies and it has been concluded that the concentration of uranium is directly proportional to the concentration of phosphorous (Bouwer and Meklveen 1978, Spalding, R. F. and Sacket 1972). Therefore, higher concentrations of uranium than normal are encountered in phosphate- rich soil (about 7-125 ppm), while the uranium content in medium-grade and high-grade ore are about 1,000-5,000 ppm, and 10,000-40,000 ppm respectively (Cember and Johnson, 2009).

In nature, natural thorium is about 4 times more abundant than uranium and contains 100% of ^{232}Th isotope (Cember and Johnson, 2009). High concentrations of thorium are commonly found in monazite minerals, (which can have thorium contents of up to 26.5%) and in zircon,up to about 13%, (UNSCEAR, 1993). A member of these three families can be simply distinguished by dividing its mass number by 4. Those nuclides which have mass numbers equal to 4n+2, 4n+3 and 4n (where n is an integer) belong to uranium, actinium and thorium series respectively. In the uranium series, there are fourteen (14) decay stages until reaching the stable ^{206}Pb while in actinium, the transformation process involves twelve (12) radionuclides with the stable end product, ^{207}Pb. Eleven (11) other radionuclides, make up the thorium chain, ending with the stable nuclide, ^{208}Pb. Figures 2.1, 2.3, and 2.4 are illustrations of decay stages observed for these three decay series.

Once an unstable nuclide emits α or β particle, the residual nucleus may attain an excited state. In order to de-excite the nucleus to its ground state, a single gamma ray or a cascade of gamma rays may be ejected. This phenomenon explains the energy difference between the initial state and the final state. For example, there are five main ɣ-ray energies emitting from a source of ^{208}Tl (in the

^{232}Th decay chain) at 277, 511, 583, 860 and 2614 keV. Other gamma-ray emission from ^{238}U, ^{232}Th, ^{235}U decay series and their daughters are shown in Table 2.1. A list of the main sources of naturally occurring radioactive nuclides are given in Table 2.2 along with some of their properties (Choppin and Liljenzin 2002).

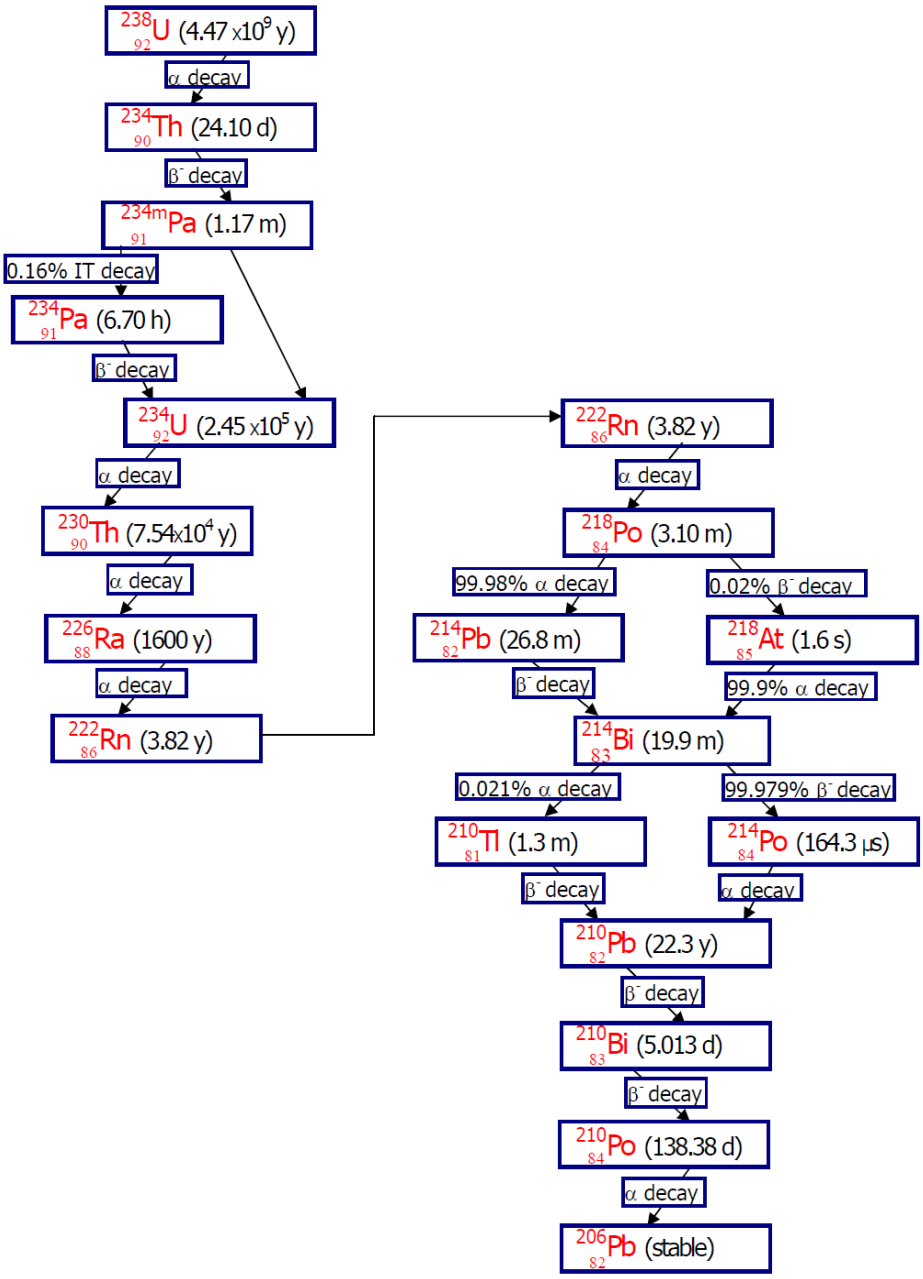

Figure 2.1: The uranium decay series

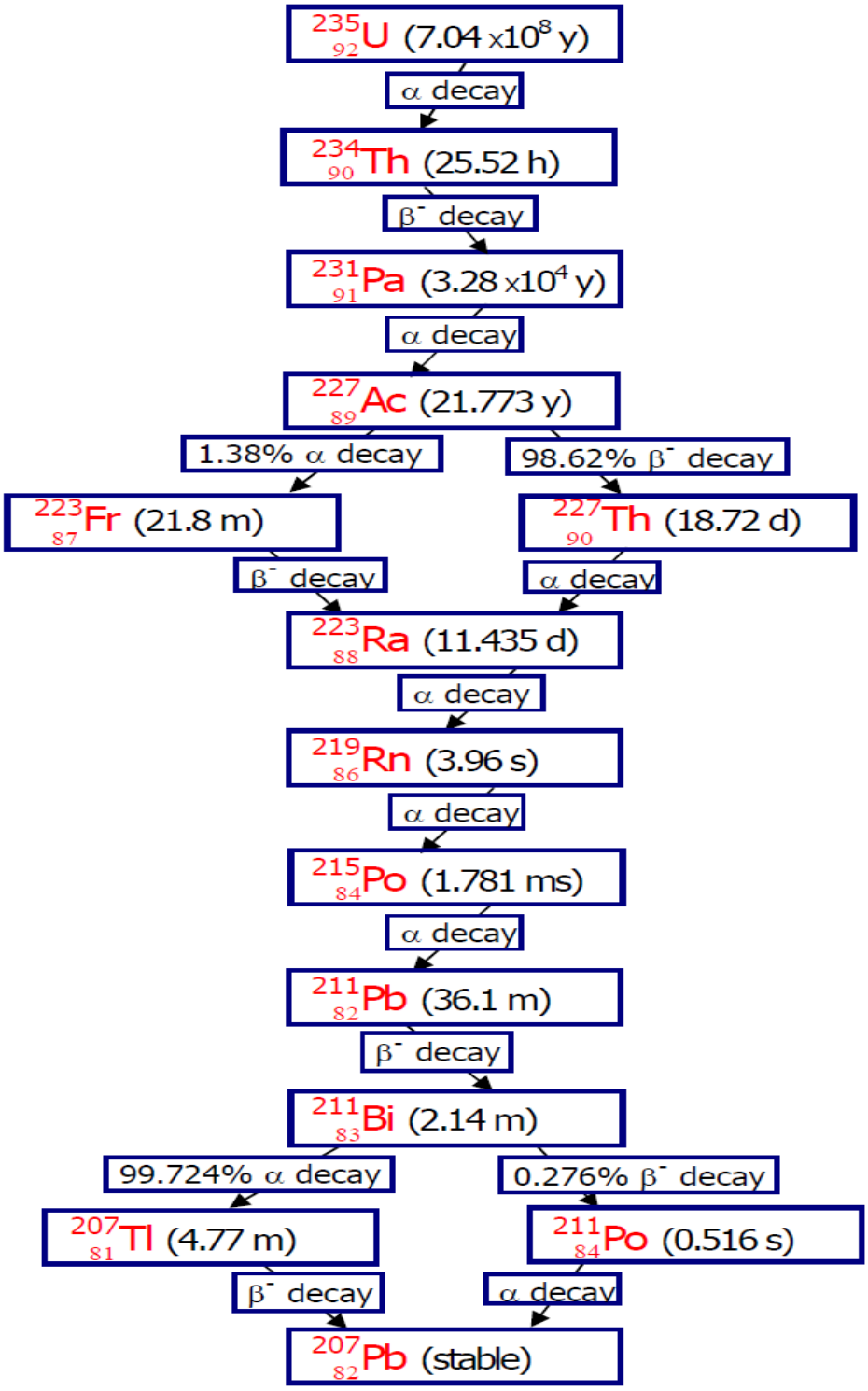

Figure 2.2: The actinium decay series.

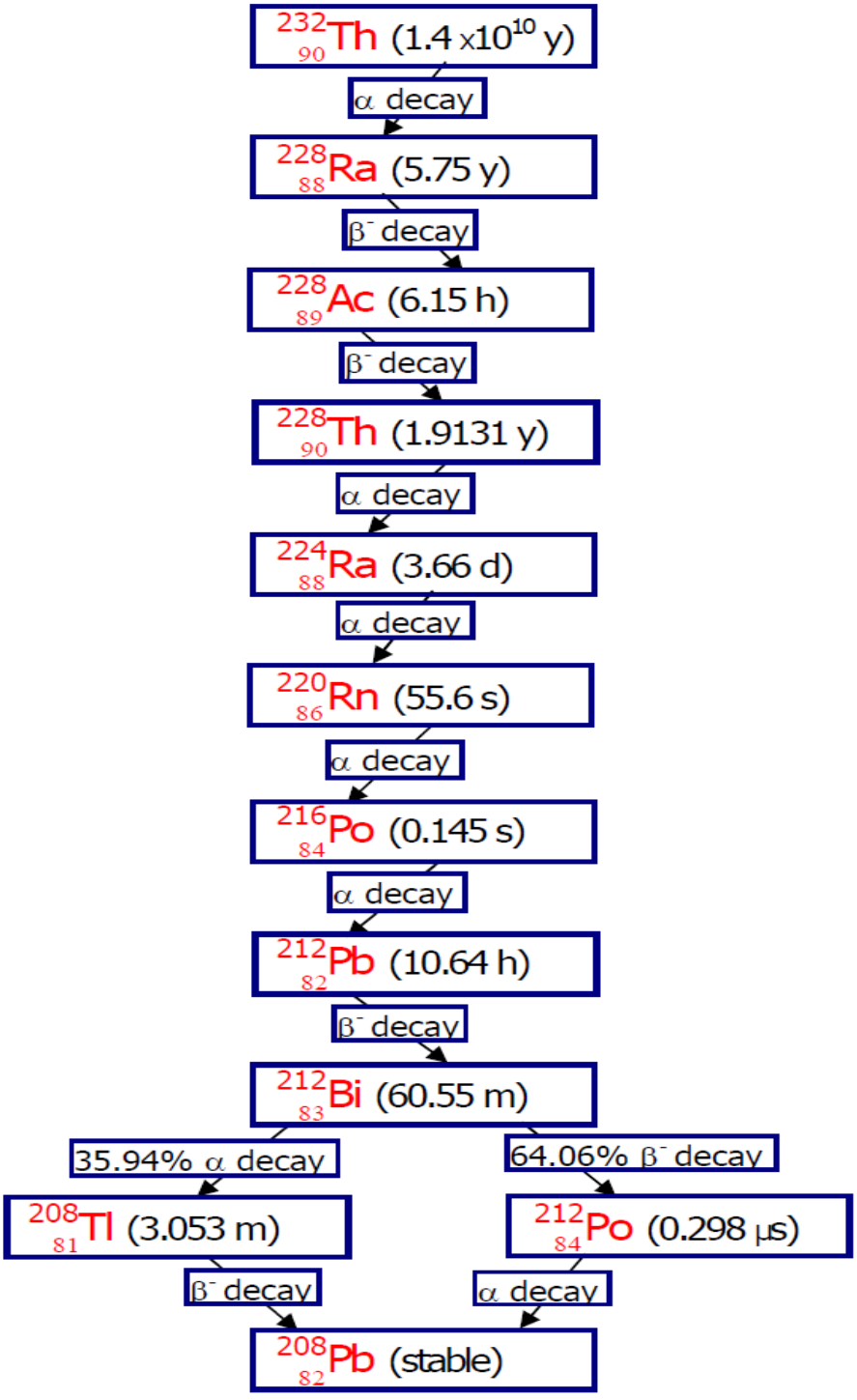

Figure 2.3: The thorium decay series

Table 2.1: The most significant gamma rays emitted by the NORM nuclides (Firestone, 1998).

Nuclide	Half-life	Decay mode	Gamma-ray energy	Emission probability
			(keV)	(%)
^{238}U series				
^{238}U	4.468 (3)x109 y	α β-	49.55 (6)	0.063 (7)
^{234}Th	24.10 (3) d		63.283 (6)	4.1 (7)
			92.370 (10)	2.42 (15)
		β-	92.793 (10)	2.39 (15)
^{234m}Pa	1.17 (3) m		1001.03 (3)	0.837 (10)
			766.38 (2)	0.294 (12)
		α α α α	742.81 (3)	0.080 (4)
^{234}U	2.455 (6)x105 y	α, β-	53.20 (2)	0.123 (2)
^{230}Th	75380 (30) y	β-	67.672 (2)	0.373 (21)
^{226}Ra	1600 (7) y		186.211 (13)	3.59 (6)
^{222}Rn	3.8235 (3) d		511 (2)	0.076
^{218}Po	3.10 (1) m	A	no γ -rays	-
^{214}Pb	26.8 (9) m	α, β-	351.932 (2)	35.1 (4)
			295.224 (2)	18.2 (2)
			241.997 (3)	7.12 (11)
^{218}At	1.6 s		no γ -rays	-
^{214}Bi	19.9 (4) m		609.312 (7)	44.6 (5)
		α β- β-	1764.494 (14)	15.1 (2)
		α, β-	1120.287 (10)	14.7 (2)
		A	1238.110 (12)	5.78 (8)
^{214}Po		-	799.7 (1)	0.0104 (35)
^{210}Tl	164.3 (20) μs		no γ -rays	-
^{210}Pb	1.3 m		46.539 (1)	4.25 (4)
^{210}Bi	22.3 (2) y		no γ -rays	-
^{210}Po	5.013 (5) d		803.10 (5)	0.00122 (4)
^{206}Pb	138.376 (2) d stable		-	-

Table 2.1: The most significant gamma rays emitted by the NORM nuclides (continued)

Nuclide	Half-life	Decay mode	Gamma-ray energy	Emission probability
			(keV)	(%)
^{232}Th series				
^{232}Th	1.405 (6)x1010 y	α β- β-	63.81 (2)	0.263 (13)
^{228}Ra	5.75 (3) y		13.52 (2)	1.6
^{228}Ac	6.15 (2) h		911.204 (4)	25.8 (4)
			968.971 (17)	15.8 (3)
			338.320 (3)	11.27 (12)
			964.766 (10)	4.99 (9)
		α α α α	463.004 (6)	4.40 (7)
		β-	84.373 (3)	1.22 (2)
^{228}Th	1.9116 (16) y		240.986 (6)	4.10 (5)
^{224}Ra	3.66 (4) d	α, β-	549.76 (4)	0.114 (17)
^{220}Rn	55.6 (1) s		804.9 (5)	0.0019 (3)
^{216}Po	0.145 (2) s	α β-	238.632 (2)	43.3 (3)
^{212}Pb	10.64 (1) h		300.087 (10)	3.28 (3)
			727.330 (9)	6.58 (6)
^{212}Bi	60.55 (6) m		1620.50 (10)	1.49 (4)
			no γ -rays	-
^{212}Po	0.299 (2) µs	-	2614.533 (13)	35.64 (6)
^{208}Tl	3.053 (4) m		583.191 (2)	30.4 (2)
			510.77 (10)	8.13 (2)
			860.564 (5)	4.47 (4)
^{208}Pb	Stable			

Table 2.2: Additional Natural Occurring Radioactive Nuclides (Firestone, 1998, Choppin and Liljenzin, 2002 and NCRP, 1987)

Nuclide	Half-life (y)	Decay mode	Isotopic Abundance (%)	Typical crustal concentration (Bq.kg-1)
^{40}K	1.26×10^{9}	β- , EC	0.0117	630
^{50}V	$> 1.4 \times 10^{17}$	β- , EC	0.25	2×10^{-5}
^{87}Rb	4.8×10^{10}	β-	27.83	70
^{113}Cd	9×10^{15}	β-	12.2	$< 2 \times 10^{-6}$
^{115}In	5.1×10^{14}	β-	95.7	2×10^{-5}
^{123}Te	1.3×10^{13}	EC	0.905	2×10^{-7}
^{138}La	1.1×10^{11}	EC, β-	0.089	2×10^{-2}
^{144}Nd	2.1×10^{15}	A	23.8	3×10^{-4}
^{147}Sm	1.06×10^{11}	A	15.1	0.7
^{152}Gd	1.1×10^{14}	A	0.2	7×10^{-6}
^{176}Lu	3.6×10^{10}	β-	2.61	0.04
^{174}Hf	2.0×10^{15}	A	0.16	2×10^{-7}
^{187}Re	4×10^{10}	β-	62.6	1×10^{-3}

The similarity of the three families is that each series contains one gaseous member from the element, radon; these are called radon (^{222}Rn, $T_{1/2} = 3.825$ d), thoron (^{222}Rn, $T_{1/2} = 55.6$ s), and actinon (^{219}Rn, $T_{1/2} = 3.96$ s) for the uranium, thorium and actinium series respectively. Since ^{220}Rn and ^{219}Rn decay away rapidly, the health hazard from ^{222}Rn gas is the most important of these to be considered. Inhalation of contaminated dust particles causes deposition of radioactive radon progeny in the lung and brings about an internal exposure. Non-gaseous radioactive daughter nuclei produced by ^{222}Rn when accumulating in the lungs give rise to a health effect of about 500 times larger than that from ^{222}Rn itself (Cember and Johnson, 2009) and ^{214}Po and ^{218}Po which are the decay products of radon can also catalyse cancer and damage cell tissue. Radon gas is an inert radioactive gas which is both colourless and odourless. It is easily spread through the air relying on various factors such as diffusion, convection processes, surface conditions, temperature and wind speed (Van der Stritch and

Kirchmann 2001). The concentration in indoor air depends on several factors such as underlying soil and rocks, ventilation in the buildings, and meteorological factors affecting the flow rate into buildings (Theodorsson, 1996). Radon is not only contained in some natural gas and oil supplies but is also present in confined spaces and ground water. It can enter buildings from soil and rocks, from building materials and tap water. High radon exposure is found in many places around the world, particularly in areas with geothermal or volcanic activity and also in caves and mines. A relationship between the weather conditions and radon levels had been discovered by various British researchers. In the cold season with high pressure conditions (i.e. cave system) the radon levels tend to increase by orders-of-magnitude. The average of ^{222}Rn concentration in outdoor air reported from several countries may be taken normally to be in the range of 4-19 $Bq.m^{-3}$ (Theodorsson, 1996).

There is a fourth decay series which is headed by ^{241}Pu, called the neptunium series. ^{241}Pu is an artificial radionuclide made in the laboratory by neutron irradiation of the reactor-produced ^{239}Pu (Cember and Johnson 2009). Even the longest half-life of the member in this series, ^{237}Np ($T_{1/2} = 2.2 \times 10^6$ yrs) is short enough to have decayed away since the birth of the earth and no longer found in nature, apart from residues from atomic weapons testing. The neptunium decay series are shown in Figure 2.4.

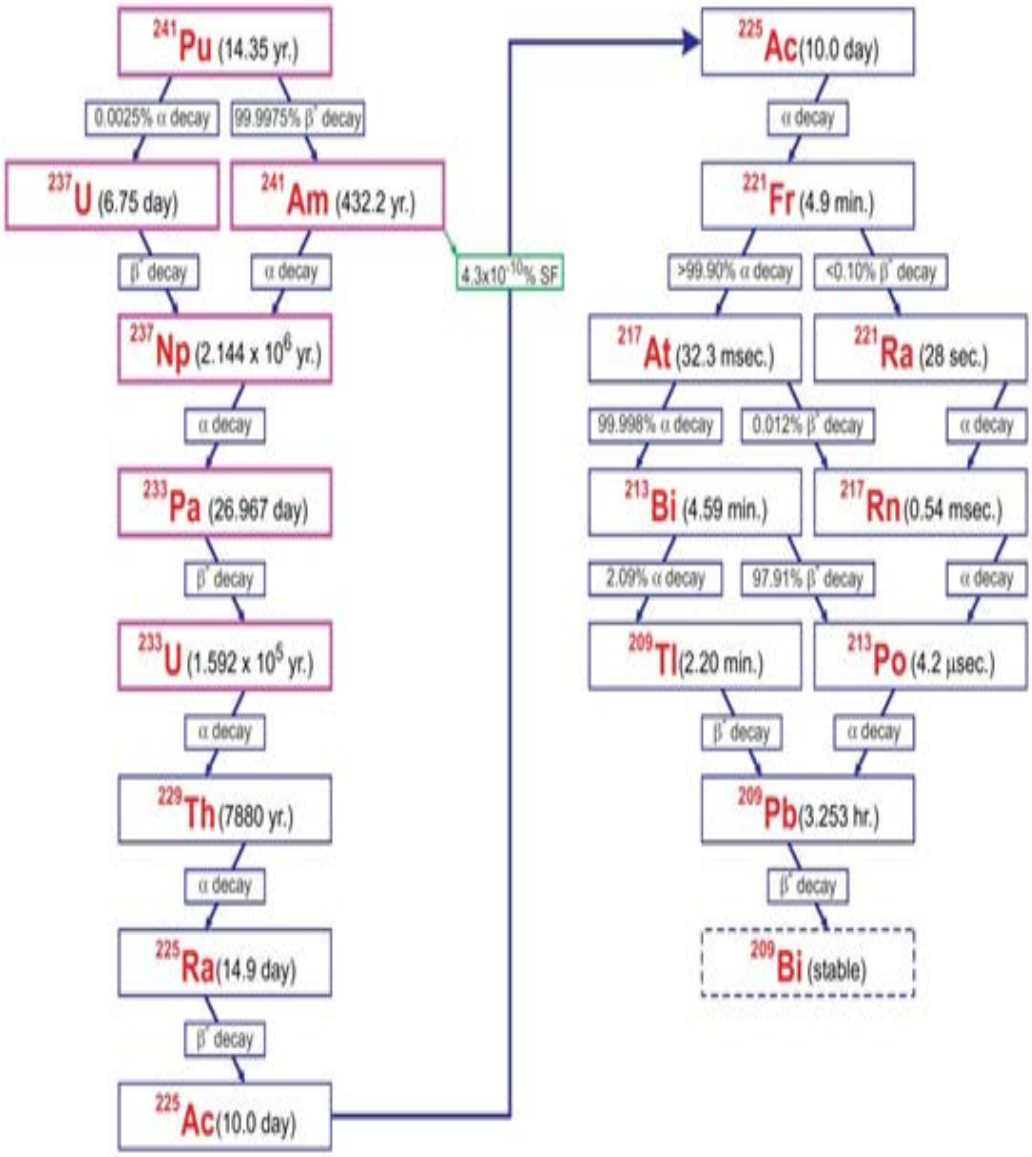

Figure 2.4: The neptunium decay series (Health, 1998).

In addition, ^{40}K, a non-series natural radionuclide with a half-life of $1.28x10^{9}$ years, is common in all types of rock, with a variation of concentrations related to those in the underlying rock. In nature, natural potassium contains only 0.0118% of ^{40}K (Theodorss, 1996). However, with an elemental abundance more than 10^{4} times that of uranium and thorium by weight in soil and rock, ^{40}K contributes to the dose received by NORM at a level comparable to that from the ^{238}U and

^{232}Th decay chains. The decay process of ^{40}K involves β^- emission (89%) and electron capture (EC) (11%). The β^- end-point energy is 1.312 MeV and a gamma ray at energy of 1.461 MeV is emitted following the electron capture decay branch, as shown in Figure 2.5.

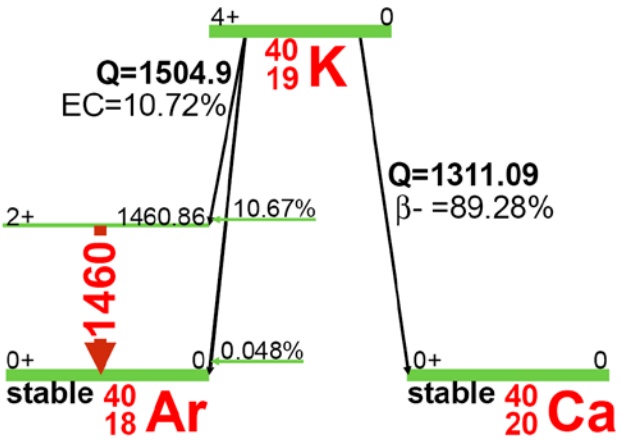

Figure 2.5: Decay scheme of ^{40}K (Health, 1998).

The concentration of ^{238}U, ^{232}Th, ^{226}Ra and ^{40}K in typical rocks and soils reported by NCRP and in other media are given in Table 2.3 and Table 2.4 respectively.

Natural radioactivity has also been investigated in seawater with the total amounts estimated to be $4.3\text{x}10^{12}$kg (53 EBq) for ^{238}U, and $6.9\text{x}10^{10}$kg (0.3 EBq) for ^{232}Th. The amount of ^{40}K is deduced to be $7.4\text{x}10^{13}$kg corresponding to the activity of $1.94\text{x}10^{4}$ EBq which is the major contribution from radioactive source in the oceans (Choppin, and Liljenzin 2002).

Table 2.3: Ranges and averages of the concentrations of ^{40}K, ^{232}Th, and ^{238}U in typical rocks and soils(NCRP, 1987)

Rock type	40K		232Th		238U	
	% total	Bq/kg	ppm	Bq/kg	ppm	Bq/kg
Igneous rocks						
Basalt (crustal ave.)	0.8	300	3–4	10–15	0.5–1	7–10
Mafic	0.3–1.1	70–400	1.6, 2.7	7, 10	0.5, 0.9	7, 10
Salic	4.5	1100-1500	16, 20	60, 80	3.9, 4.7	50, 60
Granite (crustal ave.)	>4	>l000	17	70	3	40
Sedimentary rocks						
Shale sandstones	2.7	800	12	50	3.7	40
Clean quartz	<1	<300	<2	<8	<1	<10
Dirty quartz	2a	400[a]	3–6[a]	10–25[a]	2–3[a]	40[a]
Arkosa	2–3	600–900	2[a]	<8	1–2[a]	10–25[a]
Beach sands	<1	<300[a]	6	25	3	40
Carbonate rocks	0.3	70	2	8	2	25
All Rocks (range)						
Continental crust (ave.)	2.8	850	10.7	44	2.8	36
Soil (ave.)	1.5	400	9	37	1–8	66

a indicates estimate in the absence of measured values.

Table 2.4: Natural concentration of some terrestrial radionuclides (Van der Stritch, and Kirchmann 2001).

Media	Activity concentration (Bq/kg)			
	^{40}K	^{226}Ra	^{232}Th	^{238}U
Soils	400	40	25	25
Granite	1000	100	80	60
Coal	<40	<20	<20	-
Fertilizers	<4000	<400	<20	-
Ground water	<1	<1	<1	<1
Seawater	10	<1	<1	0.04
Drinking-water	0.2	<1	-	0.004
Milk	47	0.003	-	-
Foodstuffs	40-300	0.01-100	-	-
Man	~60	0.03	-	0.1

2.2 Sources of Radiation Exposure

Human beings are inevitably exposed to ionising radiation either from external exposure arising from radioactive sources outside the body or internal exposure which comes from radioactive materials inside the body (Martin and Harbison, 2006 and UNSCEAR, 2008). Both external and internal radiation exposure to humans mainly arises from the natural sources. In addition to the natural sources, the use of radiation and radioactive materials by human activities is another source of radiation exposure to individuals (Martin and Harbison, 2006 and UNSCEAR, 2008).

2.2.1 Natural Sources

The sources of natural radiation exposure are cosmic radiation from the outer space and radioactive materials present in the earth's surroundings and wider environment, including the human body itself. About 85% of the average annual dose of 2.4 mSv received by the world population is from the distribution of these natural radiation sources (Lilley, 2001, and UNSCEAR, 2008). 15% of the total dose from natural sources is due to cosmic ray interactions at sea level; however, latitude and particularly altitude are the factors which give rise to dose rate variations from these environmental exposures (UNSCEAR, 2008). Exposure to cosmic rays at the cruising altitude of commercial aircraft is significantly higher than those at the sea level (Lilley, 2001, 55, UNSCEAR, 2008). In addition to cosmic-ray induced radiation, primordial radionuclides are a main contribution to the annual dose due to natural sources. These naturally occurring radioactive materials include radionuclides which belong to the uranium and thorium decay chains and natural radioactive potassium (^{40}K) are present in at least trace amounts in most geological materials in the Earth's crust (NCRP, 1975). Gamma radiation arising from these radionuclides is

the main source of natural, background, external exposure to human beings. The concentrations of such radionuclides at different places are a factor in the variation of external exposure due to gamma radiation from one place to another (UNSCEAR, 2008). Inhalation and ingestion of primordial radionuclides can give rise to irradiation of organs inside the body. Airborne radionuclides, such as ^{222}Rn from the ^{238}U decay chain, can enter the human body by inhalation and represent a significant source of internal exposure (Lilley, 2001, UNSCEAR, 2008).

2.2.2 Artificial Sources

Human activity involving the application of radiation is another source of radiation exposure to human. Some of these activities can give rise to an enhanced level of exposure from natural sources such as the discharge of radioactive materials into the environment from nuclear power plants, the global dispersion of radionuclides from the nuclear weapon testing or the atmospheric fall-out from the nuclear reactor accidents at Chernobyl (Lilley, 2001, and UNSCEAR, 2008) and more recently Fukushima. However, the main artificial source of the annual dose received by the worldwide population is the use of radiation for medical purposes (Lilley, 2001, UNSCEAR, 2008). Some special groups of people who work in industry, medicine and research may be occupationally exposed to radiation used in their work. The average dose from occupational exposure is relative small compared with the natural radiation exposure (Lilley, 2001, UNSCEAR, 2008). A summary of the annual average dose of ionising radiation and the range of artificial sources are also listed in Table 2.5.

Table 2.5: Annual average doses from all sources (in mSv) (UNSCEAR, 2008).

Source	**Annual average dose (Worldwide)**	**Typical range of individuals doses**	**Comments**
Natural sources of exposure			
Inhalation (radon gas)	1.26	0.2-10	The dose is much higher in some particular dwellings.
External terrestrial	0.48	0.3-1	The dose is higher in some geographical locations.
Ingestion	0.29	0.2-1	
Cosmic radiation	0.39	0.3-1	The dose increases with altitude.
Total of natural sources	2.4	1-13	
Artificial sources of exposure			
Medical diagnosis (not therapy)	0.6	0-several tens	Individual doses depend on specific examinations
Atmospheric nuclear testing	0.005	Some higher doses around test sites still occur.	The average has fallen from a peak of 0.11 mSv in 1963
Occupational exposure	0.005	~0-20	The average dose to all workers is 0.7 mSv. Most high exposures are due to natural radiation (specifically radon in mines)
Chernobyl accident	0.002[a]	In 1986, the average dose to more than 300,000 recovery workers was nearly 150 mSv; and more than 350,000 other individuals received doses greater than 10 mSv.	The average in the northern hemisphere has decreased from a maximum of 0.04 mSv in 1986.
Nuclear fuel cycle (public exposure)	0.0002[a]	Doses are up to 0.02 mSv for critical groups at 1 km from some nuclear reactor sites.	
Total of artificial sources	0.6	From essentially zero to several tens	Individual doses depend primarily on medical treatment

2.3 Radiation Protection and Dose Limits

Ionising radiation can damage biological organs in the human body. Many studies concerning the biological effects of radiation have been. The aims of these studies are to establish dose limits in order to protect radiation workers and members of the public from radiation exposure. Much of the knowledge of radiation effects on humans has been obtained from a group of people who survived from the atomic bombs in Hiroshima and Nagasaki and those individuals who received radiation exposure from routine work or accidents (Lilley, 2001, Cember, and Johnson, 2009). The relationship between biological effect and radiation exposure was studied by the Biological Effect of Ionising Radiation (BEIR) group in agreement with the United Nations Scientific Committee on the Effect of Atomic Radiation (UNSCEAR) and the International Commission on Radiological Protection (ICRP), as shown in Figure 2.6. Initial reports used a linear relationship between the effect and the amount of exposure (shown in curve A) as a ‘linear, no-threshold’ hypothesis. Further studies also allowed the possible hypothesis of a different trend (curve B) with the radiation exposure at very low levels not significant to cause harmful effects; this is referred to as the ‘threshold effect’. Curve C represents the hypothesis with the opposite effect, where absorbed doses of ionising radiation at low levels are more dangerous (Cember, and Johnson, 2009).

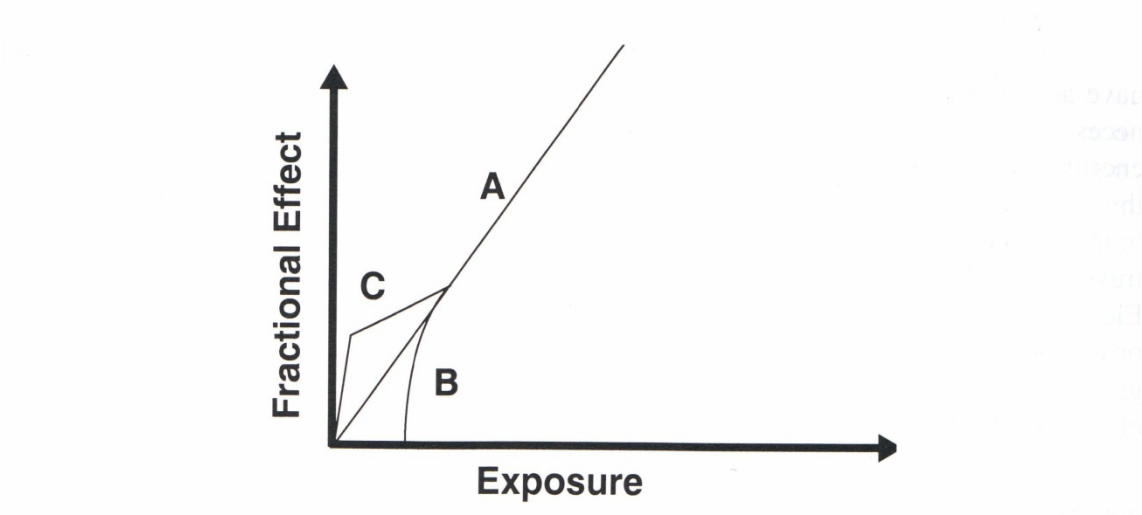

Figure 2.6: Possible, theoretical dose-response curves.

The effect of radiation exposure can be classified into deterministic effects and stochastic effects (Lilley, 2001, Cember, and Johnson, 2009 and Noz, and Maguire, 2007). The effects which are observed when organs of the body receive a certain level of dose or threshold are called deterministic effects. Below this threshold, detrimental effects are not observed. The response of the effect is similar to curve B in Figure 2.6. The severity of the effect increases with the size of the dose (Cember and Johnson, 2009 and Martin and Harbison, 2006). Stochastic effects occur randomly and the probability of occurrence is dependent on the size of the dose (Cember and Johnson, 2009 and Martin and Harbison, 2006). Cancer induction and genetic effects in future generation are thought to possibly result from these types of effects. The expected relationship between the probability of the stochastic effect and dose is along curve A in Figure 2.6.

The ICRP system of radiation protection is based on three fundamental principles: justification, optimisation and dose limitation.

The principle of justification requires that any decision that alters the radiation exposure situation should do more good than harm; in other words, the introduction of a radiation source should result in sufficient individual or societal benefit to offset the detriment it causes.

The principle of optimisation requires that the likelihood of incurring exposures, the number of people exposed and the magnitude of their individual exposure should all be kept as low as reasonably achievable, taking into account economic and societal factors. In addition, as part of the optimisation procedure, the ICRP recommends that there should be restriction on the doses to individuals from a particular source and this leads to the concept of dose constraints.

The third principle of the ICRP's system of protection is that of dose limitation. This principle requires that the dose to individuals from planned exposure situations, other than medical exposure of patients, should not exceed the appropriate limits recommended by the Commission.

As part of the system of protection, ICRP publication 103 defines three categories of exposure situations (ICRP 2007), namely: *planned exposure situations* which involve the deliberate introduction and operation of sources; *emergency exposure situations*, which require urgent action in order to avoid or reduce undesirable consequences; and *existing exposure situations*, which include prolonged exposure situations after emergencies. The ICRP recognises three categories of exposed individuals: workers, patients and members of the public. These categories of exposure are known as occupational, public and medical exposure. Occupational exposure is generally interpreted as radiation exposure of individuals as a result of their work. However, as radiation is ubiquitous, only those exposures that can reasonably be regarded as the

responsibility of the operating management are included. Medical exposure is predominantly that of patients but also includes exposures incurred by those caring for patients, other than as part of their occupation, and exposures incurred by volunteers as part of biomedical research programmes, where there is no direct benefit to the volunteer. Public exposure then incorporates all exposures other than medical and occupational.

The principles of justification and optimisation apply universally to all three categories of exposure situations (planned, emergency and existing), whereas dose limits apply only to planned exposure situations. The exception to this is planned exposure situations involving medical exposure where dose limits do not apply. In the absence of a dose limit, dose constraints assume a particular importance.

Dose constraints are used as part of the optimisation process for planned exposures. They represent a level of individual dose which should not, in normal circumstances, be exceeded. They are used in the planning process and the chosen value will depend on the circumstances of the exposure under consideration. They are not a limit and do not represent a demarcation between safe and dangerous levels of radiation exposure but are used, prospectively, as a tool for optimisation. For planned exposures that have a dose limit associated with them, dose constraints should be lower than the pertinent dose limit.

Dose limits recommended by ICRP are shown in Table 2.6.

Table 2.6: ICRP 103 recommended dose limits in planned exposure situations (ICRP 2007).

Type of limit	Occupational, mSv in a year	Public, mSv in a year
Effective Dose	20, averaged over 5 years, with no more than 50 mSv in any one year	1 (exceptionally, a higher value of effective dose could be allowed in a year provided that the average over 5 years does not exceed 1 mSv in a year)
Equivalent dose to lens of the eye	150	15
Equivalent dose to skin	500	50
Equivalent dose to hands and feet	500	-

For occupational exposure, the annual effective dose that the whole body is uniformly irradiated is limited to 20 mSv averaged over a defined period of 5 years to limit the probability of stochastic effects. The dose can be allowed to be over 20 mSv but cannot exceed 50 mSv in any single year. The dose limit of a member of the general public is set to be lower than a group of radiation workers, at 1 mSv per year. To prevent deterministic effects, occupational equivalent dose limits of 500, 500 and 150 mSv per year are recommended for the skin, the hands and the feet, and the lens of the eye, respectively. The annual equivalent doses for individual members of the public are limited to be 15 mSv for the lens of the eye and 50 mSv for the skin (Noz and Maguire, 2007, ICRP, 2007 and Martin and Harbison, 2006).

2.4 Existing Exposure Situations

There are many types of existing exposure situation. For example, aircraft crew exposure to cosmic radiation is an existing exposure situation. The cosmic ray dose rate exists, dependent upon altitude, geographical location, etc. Likewise, exposure to radon in dwellings and workplaces is, for the most part, an existing exposure situation, because the naturally occurring decay chain of uranium has not been introduced deliberately.

Naturally occurring radioactive material (NORM) presents another existing exposure situation. This includes consideration of materials that are already present on the earth's surface, and the transport of naturally occurring materials from deep within the ground to the surface as a result of activity such as drilling for oil or gas.

Two other situations also fall within the general category of existing exposure situations.

These are sites that may have contamination from past activities, perhaps from long ago, which may not, in light of today's understanding and measurements, be considered acceptable. Likewise, contamination from a nuclear accident or radiation emergency eventually falls within this category; as it now exists in the environment, little can be done to modify the source, and actions have to be considered over the long term. The transition from an emergency exposure situation to an existing exposure situation continues to be an issue of considerable discussion, and is currently being examined by ICRP Committee 4 during updates to Publications 109 and 111 (ICRP, 2009a,b) in light of the experience from Fukushima Daiichi.

Existing exposure situations have a number of unique features, some of which have already been hinted at in the above discussion. First, and perhaps obvious, existing

exposure situations are ubiquitous, and there can be wide differences between different types of situation. As such, each situation needs to be characterised and considered carefully before starting to take actions for control. The time frame or taking protective actions is not urgent, and characterisation is important to the process of justifying and optimising the recommended actions.

Control of the exposure to individuals is mainly through the pathways, as the source itself will not, in many cases, be amenable to direct control and modification. This does not mean that actions on the source are excluded, and consideration can be given to such actions when it is reasonable. Likewise, because of the wide variability, there may be a large distribution in individual exposures. This has been seen many times, such as in the contaminated zones in Chernobyl where individual habitats and locations, even within a single village, resulted in widely variable individual exposures.

The ubiquity of existing exposure situations means that workers may be receiving exposures that are adventitious, and not part of the specific work that is being done. Further, the sources may not be under the control of the operating management or employer because the source exists within the environment. In many situations with NORM, there may be a lack of experience with radiation protection, or even a lack of awareness that exposures are occurring.

The lack of existing radiation protection culture can make the introduction of control measures more difficult to accept by the individuals who are being exposed. However, it is these individuals, be they workers or simply members of the public, who are living in the existing exposure situation who can have the greatest influence on their own exposure. Informed personal behaviours, based on information, support,

and knowledge, can be one of the most significant mechanisms to reducing the risk to these individuals. This individualised action has been referred to as ‘self-help’ protective actions. Finally, existing exposure situations are unique because they require a long term perspective. The sources exist, are characterised, and actions are taken.

This does not mean that the situation goes away. Instead, this is an ongoing process, and it is important to continue to consider the source, the protective actions, and what might be reasonable and possible to improve the situation further over time.

The introduction of the three exposure situations in Publication 103 (ICRP, 2007) was designed to emphasise the commonality of the approach to radiation protection, irrespective of the circumstances. Most are familiar with the classic approach when the introduction of the source is planned. A dose limit controls the sum of all the exposures of an individual. Further, a restriction of the exposure from a particular source to a particular individual serves as a boundary of what is considered as acceptable in planning the exposure and optimising the protection.

2.5 Review of Multivariate Statistical Analysis of Environmental Data

Multivariate exploratory analysis of data has been used in various studies to derive useful information from large data sets and variables supplied by analytical techniques. Voncina *et al.* (2007) applied multivariate analysis (HCA, PCA and LDA) to radionuclide levels in relation to pH, temperature, time, and nine (9) other physical chemical parameters of ground waters from 214 wells around Slovenia in order to monitor their general pollution, identify pollution sources and to plan pollution prevention measures. The study enabled the opportunity to follow the quality of ground waters from different wells at different times of the year. Farmaki

et al. (2012) have proposed a new optimization procedure for sampling and monitoring the quality of water for domestic and industrial supply to the city of Athens, Greece based on multivariate exploratory analysis. They achieved this by applying supervised and unsupervised multivariate pattern recognition techniques to physicochemical data sets of water reservoir sources.

Chemical compositional information of Instrumental Neutron Activation Analysis (INAA) has been combined with multivariate techniques to create a geographical classification of pottery sherds from the South East of USA by Pizarro *et al.* (2008). The application of multivariate exploratory analysis combined with variables selection and data pre-treatments is therefore useful in recognizing compositionally homogeneous groups of samples that may be associated with different geographical sites.

A study of major and trace elements, ^{18}O, ^{2}H, ^{3}H, ^{13}C, ^{14}C and strontium isotopes combined with multivariate analysis and remote sensing data have been used to better understand the complex groundwater flow pattern and water-rock interactions in the tectonically active Ethiopian Rift Valley (Osenbrueck *et al*., 2013). The study indicates that groundwater flows from the escarpments into the rift valley, complying with the general hydro -chemical evolution towards $NaHCO_3$ type ground water. Additional information on contributing groundwater components and processes were obtained from a PCA of the hydro-chemical and isotopic data.

The applicability of multivariate data analysis to extract latent relationships in EDXRF spectral data, and the feasibility of forming a chemical compound classification based on characteristic fluorescence and scattered X-ray radiation has been demonstrated (Keslle*r et al*., 2002). PCA was exploited to distinguish between

spectra from different chemical compounds and also played an important role in the estimation of influences of different physical and technical parameters on spectra of different chemical compounds without packing. Goraieb *et al*. (2006) used X-ray fluorescence (XRF) spectroscopy and multivariate data analysis to distinguish types of Portland cements as well as quantify some of their constituent elements. The cement samples were classified by their distinct calcium concentrations and their origins defined by means of PLS.

Direct differentiation of ionic species in different matrices has been achieved through application of multivariate data analysis on spectral data (Oliveira *et al*., 2010). The study achieved direct speciation of chromium (Cr-III and Cr-VI) using conventional X-ray spectrometry with calculated limits of detection and quantification being lower than 17 and 50 ppm for the two ionic species respectively.

It can be seen from these studies that the range and complexity of problems that can be solved by analytical spectroscopy may be increased by application of multivariate data analysis e.g. chemometrics. Chemometrics is a chemical discipline that uses mathematical and statistical procedures to provide maximum information by analyzing data obtained from analytical techniques (Kurt and Peter, 2008). Chemometrics is most popular in the application of multivariate data analysis of complex sample matrices. Chemometrics enables extraction of relevant physical and chemical information from extensive and complex multivariate data such as spectroscopic measurements. In this study, multivariate chemometrics has been used to analyze gamma-ray spectrometric data of beach sands from the coastline of Ghana for purposes of classification and pattern recognition.

2.6 Multivariate Statistical Analysis

Multivariate statistical analysis is a promising tool to investigate the interrelationship between different parameters. It becomes necessary to analyse comprehensive data sets of sand samples in simultaneous manner to figure out relations between the parameters in question. Some authors have well developed and presented the methods of classical multivariate statistics such as Swan and Sandilands (1995), Reyment and Savazzi (1999), Davis (2002), Wackernagel (2003). The requirement for a fresh approach to multivariate statistics is caused by three recent development: (i) many classical methods exhibit poor results when dealing with large and complex data sets; (ii) the questions on a large data set is different from those of a small data set in previous time; and (iii) numerous recent improvements in computational power and equipment.

The aim of this section is to present the state of the art methods that have been developed in an attempt to discover any hidden patterns or structures of the data set. The goal of experimental science is the understanding and exploration of unknown relations including natural laws. To explore these laws, the methods of classification, comparison and prediction are used. In classification, relevant parameters have to be measured. Methods of hypothesis tests and statistical models have been used for comparison and conjecture. A display of scatterplot of two variables is well known.

However, when dealing with more than two variables, it becomes more difficult to visualize the multivariate data distributions.

2.6.1 Data Structure

A starting point for all multivariate statistical algorithms is a matrix in which rows represent the objects and columns the variables. In this study, an object represents an investigated sand sample. As a matter of convention, the rows of a data matrix represent sand samples and the columns represent the properties of these samples. In multivariate statistics the number of samples n should be larger than the number of properties p. The data matrix is of rectangular shape $n \times p$. The various properties of a sample are normally distributed in the range of magnitude. The manipulation of centering or normalizing of the data matrix should be done prior to the multivariate statistical analysis.

2.6.2 Measurement of proximity

Measures of proximity are of two types: similarity and dissimilarity (distance). These measures indicate how similar or dissimilar objects are to each other. Upon the type of data, several authors have discussed various similarity and dissimilarity definitions together with associated problems (Gower, 1985, Baulieu, 1989, Jackson et al., 1989 and Gordon, 1999). The choice of a proximity measure depends upon the problem at hand. Suppose a data set of n objects has dissimilarities δ_{rs} measured between all pairs of objects, a configuration of n points representing the objects is sought in a p dimensional space. Each point represents one object, with the r^{th} point representing object r. Let the distances between pairs of points be d_{rs}. The aim of visualization is to find a configuration such that the distances d_{rs} match as well as possible the dissimilarities δ_{rs}. The different notions of “matching” give rise to different techniques of multidimensional scaling (MDS).

2.6.3 Euclidean metrics

These metrices correspond to the straight line distances in Euclidean space. In a univariate example, the Euclidean distance between two values is the arithmetic difference. In a bivariate case, the minimum distance between two points is the hypotenuse of the right-angled triangle in the two-dimensional space. For three variables the hypotenuse extends through three-dimensional space. Although it is difficult to visualize, an extension of Pythagoras theorem gives the Euclidean distance between two points in *n*-dimensional space:

$$\delta_{rs} = \left\{ \sum_{i-1}^{P} (x_{ri} - x_{si})^2 \right\}^{1/2} \qquad \text{(Eq. 2.1)}$$

A weighted Euclidean distance considers varying weights for different properties:

$$\delta_{rs} = \left\{ \sum_{i-1}^{P} w_i (x_{ri} - x_{si})^2 \right\}^{1/2} \qquad \text{(Eq. 2.2)}$$

2.6.4 Mahalanobis distance

The Mahalanobis distance is a generalised form of an Euclidean distance which weighs variables using the sample variance-covariance matrix **R**. Because the covariance matrix is used, the correlations between variables are taken into account. The Mahalanobis distance is normally used to measure the difference between the means of two multivariate groups. It can be defined as a similarity measure between two vectors $\mathbf{x}_r$ and $\mathbf{x}_s$ of the data matrix with the covariance matrix **R**:

$$\delta_{rs} = \{[x_r - x_s]^T R^{-1} [x_r - x_s]\}^{1/2} \qquad \text{(Eq. 2.3)}$$

2.6.5 Cosine coefficient

The cosine coefficient expresses the dissimilarity between object ***a,*** and object ***b*** by regarding each as a vector defined in a ***p*** dimensional space. This is a non-Euclidean, pattern similarity metric. The cosine of the angle between two vectors is identical to their correlation coefficient. However, unlike a normal correlation calculation the pairs of values are drawn from different variables for two cases rather than two variables from different cases. The Cosine of two objects, ***a*** and ***b,*** is defined as

$$\cos\theta_{ab} = \frac{\sum_{k=1}^{p} x_{ak}x_{bk}}{\left\{\left(\sum_{k=1}^{p} x_{ak}^2\right)\left(\sum_{k=1}^{p} x_{bk}^2\right)\right\}^{1/2}} \qquad \text{(Eq. 2.4)}$$

2.6.6 Cluster Analysis

Cluster analysis and classification are both techniques of placing objects into groups or classes. The difference is that in a cluster analysis the classes are not predefined as in classification. Cluster analysis, which is the most well-known example of unsupervised learning, is a very popular tool for analyzing unstructured multivariate data. The methodology consists of various algorithms each of which seeks to organize a given data set into homogeneous subgroups, or “clusters”. A cluster is simply a collection of samples that are more “similar” to each other than they are to samples in other clusters. There is no guarantee that more than one such group can be found. In any practical application, however, the underlying hypothesis is that the data form a heterogeneous set should be separated into natural groups.

All clustering algorithms begin by measuring the similarity or dissimilarity between the samples to be clustered. Similar samples will be placed into the same cluster. It is also possible to view similarity by its inverse, the distance between cases, with distance declining as similarity increases. This leads to a general conclusion that

objects in the same cluster will be closer to each other or more similar than they are to objects in other clusters. It also means that there must be some means of measuring distance. The most obvious distances are Euclidean, which are straight lines that can be measured with a “ruler” while others, often based on similarity, are non-Euclidean.

2.6.6.1 Partitioning Methods

Partitioning techniques encounter the problem of dividing *n* samples, described by *p* variables, into a small number *k* of discrete classes. The *k*-means is one of the simplest unsupervised learning algorithms that solve the known clustering problem. The most intuitive and frequently used criterion function in partitioned clustering techniques is the squared error criterion or objective function. This algorithm aims at minimizing an objective function

$$J = \sum_{j=1}^{k} \sum_{i=1}^{n} \left\| x_i^{(j)} - c_j \right\|^2 \qquad \text{(Eq. 2.5)}$$

Where $\left\| x_i^{(j)} - c_j \right\|^2$ is a chosen distance measure between a data point $x_i^{(j)}$ and the cluster center c_j. The objective function *J* is an indicator of the distance of the n data points from their respective cluster centers. The algorithm is composed of the following steps that are iterated until a solution is found:

1. Choose *k* cluster centers that coincide with k randomly defined points. The initial clusters could be random or based on some “seed” values.
2. Repartition by assigning each samples to the closest cluster center.
3. Re-compute the cluster centers as centroids.
4. Repeat steps two and three until convergence is achieved. The endpoint will be the minimum of the objective function *J*.

The *k*-means algorithm does not necessarily find the optimal configuration, corresponding to the global objective function minimum. The algorithm is also significantly sensitive to the initial randomly selected cluster centers. The *k*-means algorithm can be run multiple times to reduce this effect.

2.6.6.2 Hierarchical method

Hierarchical techniques are the most widely applied clustering techniques in the earth sciences. Gordon (1987) reported an excellent review on hierarchical classification. This method joins the most similar observations, then successively connects the next most similar ones to these. The graphic display of the complete clustering process is a dendrogram. The nodes of the dendrogram represent clusters, and the lengths of the stems (heights) represent the distances at which clusters are joined.

Given a set of n items to be clustered, and an $n \times n$ distance matrix, the basic process of hierarchical clustering runs as follows:

1. Assign each item to a cluster, each cluster contains just one item. Let the distances between the clusters be the same as the distances between the items they contain.
2. Find the closest or most similar pair of clusters and merge them into a single cluster, so that now we have one cluster less.
3. Calculate the distances between the new cluster and each of the old clusters
4. Iterate steps 2 and 3 until all items are clustered into a single cluster of size n

Step 3 can be done in different ways, which is what distinguishes single-linkage from complete-linkage and average-linkage clustering. In single-linkage clustering one considers the distance between one cluster and another cluster to be equal to the shortest distance from any member of one cluster to any member of the other cluster.

If the data consists of similarities, we consider the similarity between one cluster and another cluster to be equal to the greatest similarity from any member of one cluster to any member of the other cluster. In complete-linkage clustering, we consider the distance between one cluster and another cluster to be equal to the greatest distance from any member of one cluster to any member of the other cluster. In average-linkage clustering, we consider the distance between one cluster and another cluster to be equal to the average distance from any member of one cluster to any member of the other cluster.

This type of hierarchical clustering is called agglomerative because it merges clusters iteratively. There is also a divisive hierarchical clustering which does the reverse by starting with all objects in one cluster and subdividing them into smaller pieces. Divisive methods are not generally available, and have been rarely applied in earth sciences.

2.6.7 Principal Component Analysis (PCA)

Principal Component Analysis (PCA) is the most widely used method of multivariate data analysis due to its simple algorithm and straightforward interpretation. The major goal of PCA is to reveal hidden structures in a data set. In geosciences, PCA can be used for (i) Reducing the dimensionality of the data, (ii) Multivariate outliers detection, (iii) Decoding a correlation matrix, (iv) Identifying underlying factors, (v) Detecting intrinsic correlation, and (vi) Preparing the data for further analysis using other techniques (Jolliffe, 2002, Wackernagel, 2003).

Consider a data matrix $\mathbf{X}_{n\times p}$ of n sand samples and p variables. If the variances are significantly different in the data or variables measured in different dimensions, the data matrix should be standardized by subtracting the means of each row and scaling

each row by dividing by its standard deviation. The variance-covariance matrix can be calculated as:

$$R = X^T X \qquad (Eq.\,2.6)$$

The interrelationships between a data matrix and the eigenvalues and eigenvectors of its two cross product matrices are expressed in the singular value decomposition (SVD), well known as Eckart-Young theorem:

$$X = U\Sigma V^T \qquad (Eq.\,2.7)$$

with $U_{n*n}\ and\ V^T_{p*p}$, the transpose of **V**, being unitary matrices. $\boldsymbol{\Sigma_{n*p}}$ is a diagonal matrix with non-negative numbers on the diagonal containing the singular values of **X**. The columns of **V** are termed the principal components or the principal component loadings in PCA literature. The fundamental characteristic of PCA is to approximate **X** by a lower rank matrix $\widehat{\mathbf{X}}$ which minimizes the residual distance $\|\mathbf{X} - \widehat{\mathbf{X}}\|$ on the basis of an approximation of the least squares criterion. The *r* dimensional Eckart Young approximation becomes more informative as:

$$\widehat{\mathrm{X}} = \mathrm{U}\Sigma_{\mathrm{r}}\mathrm{V}_{\mathrm{r}}^{\mathrm{T}} = X\mathrm{V}_{\mathrm{r}}\mathrm{V}_{\mathrm{r}}^{\mathrm{T}} \qquad (Eq.\,2.8)$$

where *r*, is the lower rank. The rows of $\mathbf{U\Sigma}_r$ give the *r* dimensional coordinates for the *n* samples, while the columns of $\mathbf{V}^{\mathrm{T}}$, the rows of **V**, give the directions of the biplots axes which will be elaborated in the next sections.

To approximate a data matrix **X**, the analysis is based on the singular value decomposition (SVD), while an approximation of the variance-covariance matrix $\mathbf{X}^T\ \mathbf{X}$ is based on the spectral eigenvalues decomposition which happens to coincide with its singular value decomposition. The variance-covariance matrix can be written as:

$$R = X^T X = \mathrm{V}\Sigma^2 V^T \qquad (Eq.\,2.9)$$

and the approximation to the variance-covariance matrix is given as:

$$\widehat{\mathrm{X}}^{\mathrm{T}}\widehat{\mathrm{X}} = \mathrm{V}_{\mathrm{r}}\Sigma_{\mathrm{r}}^2\mathrm{V}_{\mathrm{r}}^{\mathrm{T}} \qquad (Eq.\,2.10)$$

The PCA method is actually a statistical interpretation of the eigenvalues. Multiplying the data matrix **X** with the eigenvector matrix **V** results in a score matrix **Y** that contains the principal components:

$$\mathrm{Y} = \mathrm{XV} = \mathrm{U\Sigma} \qquad (Eq.\,2.11)$$

2.6.7.1 PCA Visualization in Multidimensional Space

For the graphical representation, a PCA approximation is presented in a *r*-dimensional subspace **L** of the *p* space which results from a best fitting in the least squares sense. With the *r*-dimensional subspace **L**, *n* points can be orthogonally projected on it.

This subspace is characterized by the minimum sum of squares residuals between the original points and their projections. When representing the samples relative to orthogonal axes in **L**, the coordinates of the projected points are given by

$$\mathrm{Y} = \mathrm{X_r V_r} \qquad (Eq.\,2.12)$$

If the dimension *r* = 2, the best fitting subspace **L** will be a plane of best fit. The projection of original axes on the *r*-dimensional best fitting subspace defines the bi-plot axes.

2.6.7.2 Measures of fit in PCA Method

The overall quality of approximation of the sample matrix **X** is usually measured as the ratio of the variance on the corresponding approximation to the total variance or in terms of fitted to total sums of squares:

$$\frac{Variance\ of\ the\ factor}{Total\ variance} = \frac{\sum_{i=1}^{r} \sigma_i^2}{\sum_{i=1}^{p} \sigma_i^2} \qquad (Eq.\,2.13)$$

To measure the approximating variable, a quantity termed adequacy is used to assess the approximations of the sample matrix **X**. In an *r*-dimensional approximation, the adequacy of a specific variable is defined as

$$Adequacy = \Sigma_{i=1}^{T} v_i \qquad (Eq. 2.14)$$

where v_i are the i^{th} diagonal values of $V_r V_r^T$. Axis adequacy is a measure of sums of squares of the rows of the eigenvectors matrix.

Axes predictivity is another important parameter to measure the fitting quality. It is defined as the ratio of the diagonal of the variance-covariance approximation matrix to the corresponding elements of variance-covariance matrix:

$$Predictivity = diag\left(\hat{X}^T \hat{X}\right)\{diag(X^T X)\}^{-1} \qquad (Eq. 2.15)$$

where the terms $X^T X$ and $\hat{X}^T \hat{X}$ were described in equations 2.8 and 2.10, respectively.

CHAPTER 3

THE STUDY AREA

The aim of this chapter is to describe the study area in terms of its locality, land use, topography, drainage, climate, geology and habitats.

3.1 Description of the Study Area

The coastline of Ghana comprises the sandy east coast; the central coast, which is dominantly rocky beaches interspersed with short sections of sandy beaches; and the sandy west coast (Armah and Amlalo, 1998). Two main types of coastal lagoons can be found in Ghana. These are “open” and “closed” lagoons (Armah, 1991). The open lagoons have a permanent opening to the sea and are normally fed by rivers that flow all year round. They can be found mostly on the central and western parts of the coastline where higher rainfall results in a more continuous flow of rivers and streams into the sea (Plate 3.1).

Plate 3.1**:** Rubbish from the main land deposited at the Nungua Beach after a heavy rain

3.1.1 Geology

It is believed that the coastal geological formations of Ghana were likely determined by continental drift during the Cretaceous period (about 135 million years ago), when Africa broke away from South America (Allersma and Tilmans, 1993). The geological composition consists of hard granites, granodiorites, metamorphosed lava, and pyroclastic rock. Some coastal areas are covered by Ordovician, Silurian, and Devonian sandstone and shales (Allersma and Tilmans, 1993).

The coastal zone is composed of extremely old marine sediments, which occur along the coast between Takoradi and Cape Coast and around Accra. Fresh water sediments occur in the Saltpond area, whilst much younger marine series of shale, sand stones and limestones are found in the extreme southwest and southeast of the country (Agyepong et al. 1990). The area of most rapid erosion occurs in the weaker geological formations (Figure 3.1). The area is underlain by very ancient rocks belonging to the Precambrian and Palaeozoic eras. The general topography is characterised by moderate relief. The occurrence of rock outcrops along the Ghanaian shoreline appears to be largely due to relief and change of climate (Dei, 1972).

3.1.2 Climate

Climate in the coastal zone is varied. Total annual rainfall varies from less than 875 mm in the eastern to more than 2000 mm in the western part. Minimum temperatures of about 25 degrees Celsius occur in July and August, whereas maximum temperature occurs during February to March, preceding the main rainfall season (Agyepong et al. 1990).

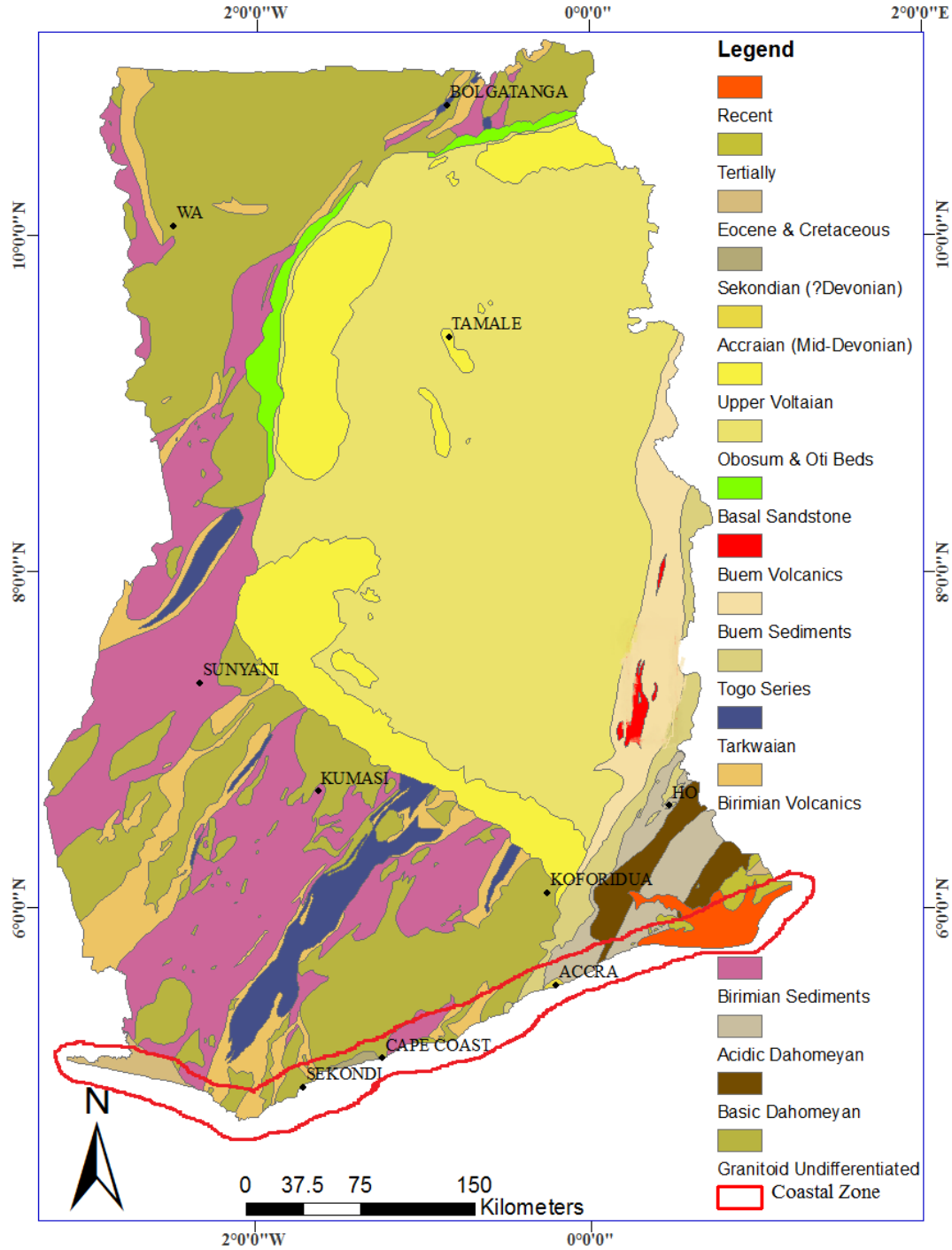

Figure 3.1: Geological Map of Ghana showing the Coastal Zone. (Modified from World Bank 1997)

3.1.3 Vegetation

The vegetation types of the coastal zone from east to west reflect the rainfall pattern (Agyepong et al. 1990). They range from coastal shrub and savannah to marginal forest to dry semi-deciduous and moist semi-deciduous forest and finally to wet evergreen forest in the extreme southwest of the country. The immediate coastal zone comprises the strand vegetation, the lagoons and marshes (Agyepong et al. 1990). The western part from the frontier with Côte d'Ivoire to Cape Coast is dominated by semi-deciduous and evergreen secondary tropical forest. The area from Cape Coast to the eastern border with Togo comprises a relatively dry zone with low-lying thickets, shrubs and savannah grassland (Armah and Amlalo, 1998). Important factors that affect the survival of vegetation in this area are wind, excessive evaporation, salt spray, saline conditions and looseness of substratum. Examples of terrestrial plants in the coastal zone are Ipomoea spp, Canavalia rosea, and Thespesia populnea (Agyepong et al. 1990).

3.1.4 Habitats

Six coastal ecosystem types occur in Ghana, namely: sandy shore, rocky shore, coastal lagoons, mangrove/tidal forests, estuarine wetlands and depression wetlands. Ecosystems found along the coast include mangroves, estuaries, lagoons beaches, mudflats, sand flats, and sea grass systems. These habitats have very important ecological and social functions. There are five coastal wetlands of international importance - Anlo-Keta, Songor, Sakumo, Densu Salt Pans and Muni. Four others may also be similarly protected: the Keta, Korle, and Amazuri wetlands and the Elmina saltpans. The coastal wetlands are traditionally exploited for agriculture, fishing, sand and salt winning, and natural products such as reeds (Gordon, 1998).

3.1.5 Animal Life

Turtles and manatees: Many parts of the coastal zone such as Ada and Shama are important nesting sites for marine turtles. Occurring species include the Leatherback (Dermochelys coriacea), the Olive Ridley (Lepidochelys olivacea) and the Green turtles (Chelonia mydas). The West Africa manatee (Trichechus senegalensis) has also been sighted in some coastal areas such as those around the lower Volta.

Birds: Sandy beaches, estuaries, lagoons and flood plains along the coast of Ghana provide feeding and roosting sites for many birds, including migratory birds. Over 80% of the total number of shoreline bird species recorded in Ghana is reportedly Palaearctic migrants (Ntiamoa-Baidu and Hepburn, 1988).

Fish: Fish is not only an important source of protein but also a source of livelihood and employment along the coast of Ghana. Marine landings are made in the Western, Central, Greater Accra and Volta Regions (Directorate of Fisheries, 2003). The marine fisheries fleets are classified as artisanal, inshore or semi-industrial and industrial (Mensah et.al, 2001). Artisanal fishery contributes most of the domestic marine fish supply such as small pelagics, especially the round sardinella, flat sardinella, anchovy and club mackerel (Directorate of Fisheries, 2003). It is responsible for over 80% of the total annual catch of small pelagic fish species (Bannerman et al. 2001). According to the 2001 census there were 9,981 artisanal wooden dugout canoes operating, most of which use 40 horse power outboard motors. The introduction of outboard engines to the canoes started in the 1950s and enabled the fishermen to move further out to sea from the coast to make bigger catches (Mensah et al. 2001). The Ghana Canoe Frame Survey estimates that there are about 124,000 fishermen operating from 334 landing sites in 195 fishing villages along the marine coast (Bannerman et al. 2001). Commonly used fishing gears are

purse seines, beach seines, set nets, drift gill nets and hook and line. Different gears are used at different times of the year to exploit different species of fish (Mensah et al. 2001). Fishing in the coastal zone by canoe fleet is directly related to seasonal upwelling that occurs in the coastal waters of Ghana. The major fishing season which stretches from June to October coincides with the major upwelling whilst the minor fishing season which is from December to February coincides with the minor up-welling. For the rest of the year fishing is poor.

The semi-industrial/inshore fleet consists of locally built wooden vessels of 8 to 37m in length with inboard engines of between 90 and 400 horse power. Most vessels can either use trawl or purse seine nets. In 2000 there were 169 inshore vessels (MOFI, 2006 and Mensah et al. 2001).

The industrial vessels are generally large, steel-hulled foreign built vessels that fish for shrimp, tuna and other species, mainly sea bream, cuttle fish and cassava fish. They include freezer trawlers and purse seiners (Directorate of Fisheries, 2003). Industrial vessels operate from Tema and also from Takoradi. About 30% of tuna landed by the tuna vessels is intended for the domestic market and 70% is exported. In 1996 there were 35 tuna vessels operating in Ghanaian waters (Mensah et al. 2001) and 9 shrimp vessels in 1998. Due to the high level of investment required, many vessels operate on a joint venture basis between Ghanaians and outside investors from Korea, France and other countries (Directorate of Fisheries, 2003). Fishing also takes place in all the coastal wetlands, especially in lagoons, and also in the brackish-water marshes in depressions (Directorate of Fisheries, 2003). The species caught in the coastal lagoons and estuaries are tilapia (Cichloidae) mostly the black chinned tilapia (Saratherodon melanotheron), horse mackerel and the mullets. Oyster and crabs (Callinectes) are also caught here (Agyepong et al. 1990). The

most important lagoon fish, tilapia, accounts for about 98% of the catch (Directorate of Fisheries, 2003).

3.1.6 Salt Production

Salt production is an important activity along the coast of Ghana (Agyepong et al. 1990). It is carried out in the flat areas along the coast, especially in the Keta and Songor lagoons, Ada, Ningo, Weija-Accra, Prampram, Apam, Cape Coast, Iture and Elmina areas. In most cases the salt is collected from the lagoon floors during the dry season when high evaporation leads to the precipitation of salt (Directorate of Fisheries, 2003). The salt is marketed locally and in neighbouring countries. Commercial exploitation is being encouraged especially under the government's economic drive of Presidential Special Initiative on Salt.

3.1.7 Mineral Resources

Deposits of limestone, silica, feldspar, kaolin and other minerals have been identified within the coastal belt (Laing, 1991). Sand from these beaches are used by the local people for making concrete bricks and sand-cement mixture needed for plastering walls (Plate 3.2). However these minerals do not occur in commercial quantities. On the other hand, crude oil has been discovered in commercial quantities.

Plate 3.2: Sand, from the Teshie beach, used by the local people for making sand-cretes.

Plate 3.3**:** Holiday makers and Tourists at the Labadi Pleasure Beach.

3.1.8 Tourism

Since the late 1980s, tourism has received significant consideration in the economic development strategy of Ghana. The coastal zone has played a crucial role in attracting both local and international tourists (Kuma, 2004) (Plate 3.3). Tourist attractions include the animal life, beaches, physical infrastructure such as hotels, beach resorts and forts and castles, cultural events and festivals (Tweneboah, 2001).

CHAPTER 4

MATERIALS AND METHODS

This chapter deals with the sample collection and calibration of the HPGe based spectrometer for activity measurements as well as the determination of specific activities, dose rates, annual effective dose due to beach sands and the associated hazard indices. The multivariate statistical procedures used in the analysis of the spectral and measured radiological data are also explained.

4.1 Sample Collection and Preparation

Ten (10) popular resort or landing beaches in each of the four coastal regions (except the Central Region, where eleven beaches were selected) were considered as sampling sites, taking into account; accessibility to the beaches, the time frame of the research, equipment and logistic available. Five (5) replicate samples of beach sand were collected at random positions from each site at depths between 5 and 25cm. In the laboratory, the sand samples were spread on trays and allowed to dry at room temperature and to remove excess moisture, for 14 days. Samples were then oven-dried at 105°C for 24 hours (with a slow-airflow drying cabinet), ground, homogenised, and screened with a size 20 mesh. They were then packed into Marienelli beakers, of 1000 cm^3 volume each. Before measurements, the containers with the samples were kept sealed for 30 days, with the assumption that the long-lived parent nuclides will establish secular equilibrium with their respective short–lived daughters (TRACERCO, 2007).

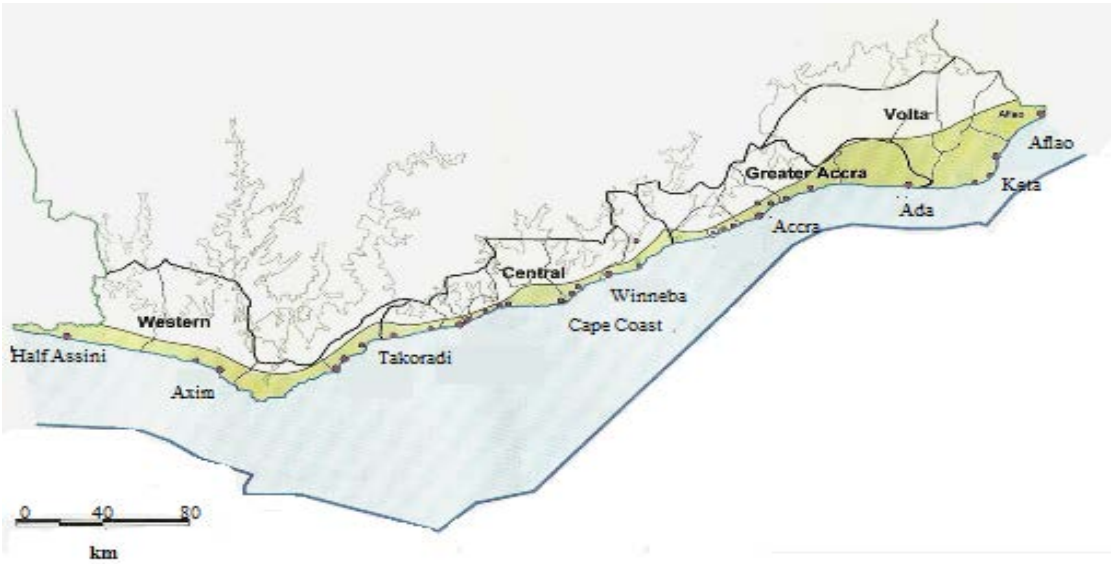

Figure 4.1: Map of Coastal Zone of Ghana showing the study area and some sampling points. (Modified from World Bank 1997)

4.2 Instrumentation

Activity measurements were performed by gamma-ray spectrometry. The gamma spectrometer used for this work consist of a High Pure Germanium Detector (HPGe), with properties shown in Table 4.1, cooled by 25 litre liquid nitrogen in a dewar. The detector assembly is coupled to a desk top computer provided with Maestro 32 MCB configuration software for spectrum acquisition and evaluation. To reduce the background radiation, the detector is located inside a cylindrical lead shield of 5 cm thickness, internal diameter of 24cm and height of 60cm. The lead shield is lined with various layers of copper, cadmium and plexilglass (to absorb X- rays generated in the lead) each of 3mm thick.

Table 4.1: Properties of High purity germanium detector (HPGe)

Detector specification	**Physical characteristics**	**Electrical characteristics**
Model GR 2518-7500sl	Geometry: coaxial one open ended	Depletion voltage (-) 2500 vdc
Serial no b95529	Diameter : 54mm	Recommended bias voltage (-) 300 vdc
Relative efficiency 25%	Length : 53mm	Leakage current at recommended bias : 0.0nA
Resolution 1.8 kev (FWHM) at 1.33 Mev gamma-ray of ^{60}Co – 1.8 keV	Distance from window 5mm long	Pre amplifier test point at recommended voltage (-) 1.0vdc
Peak/Compton - 55:1		

Plate 4.1: The High Pure Germanium Detector assembly used for analysis of the samples of beach sand at the Ghana Research Reactor – 1.

4.2.1 Calibration of the γ-Spectrometer

Prior to the analysis of the samples, energy and efficiency calibrations were performed to enable identification and quantification of the radionuclides. The detector system was calibrated using the multinuclide standard solution. The standard was measured in the 1.0 litre Marinelli beaker.

The standard used for the energy and efficiency calibration consisted of a liquid mixed radionuclide solution with the following corresponding energies; ^{241}Am (59.54 keV), ^{109}Cd (88.03 keV), ^{57}Co (122.06 keV), ^{139}Ce (165.86 keV), ^{203}Hg (279.20 keV), ^{113}Sn (391.69 keV), ^{85}Sr (514.01 keV), ^{137}Cs (661.66 keV), ^{60}Co (1173.2 keV and

1332.5 keV) and ^{88}Y (898.04 keV and 1836.1 keV): and was supplied by the IAEA. The measurement geometry used for samples were the same as that of the standard.

In order to determine the background radiation in the environment around the detector, an empty sealed Marinelli beaker was counted in the same manner and in the same geometry as the samples. The measurement time used for the background was 43 200 s. The background spectra were used to obtain the net peak area of gamma rays of measured isotopes. A dedicated software program, Maestro 32 MCB, was used to carry out the online analysis of each measured gamma-ray spectrum.

4.2.2 Energy Calibration

One of the essential requirements in nuclear spectroscopy measurement is the ability to identify the photo peaks present in a spectrum produced by the detector system (IAEA, 1989). This is achieved by carrying out energy calibration of the detection system.

Energy calibration was performed by matching the energies of the principal gamma-rays in the spectrum of the standard reference material to the channel number of the spectrometer. This was done both manually and with the computer. The equation relating the energy and the channel number is given by the expression (Cember and Johnson, 2009).

$$E_\gamma = A_0 + A_1 CN \qquad \text{(Eq. 4.1)}$$

where E_γ is the energy, CN is the channel number for a given radionuclide, and A_o and A_1 are calibration constants for a given geometry. A graph of energy against channel was plotted as shown in Figure 3.3.

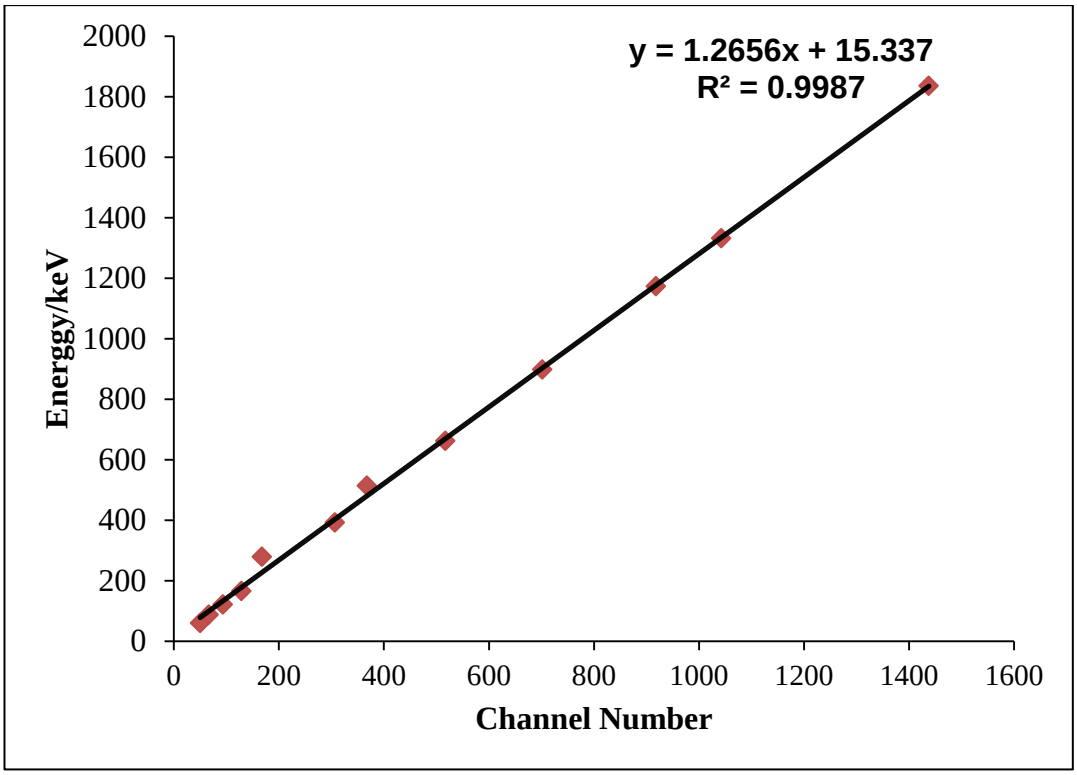

Figure 4.2: Energy calibration Curve.

Once energy calibration is performed, the next step in the sequence of spectrum analysis would be the determination of the resolution. The resolution is defined by the parameter FWHM (full width at half height of the photopeak), and assuming that photopeak fits a Gaussian, the value will take this parameter FWHM = 2.35σ being assigned the standard deviation σ from software to the Gaussian distribution.The resolution of Ge detectors usually comes (originally) specified because it provides information about the spacing capability of the photopeaks presenting a particular system. Generally nominal resolutions often used are: ^{55}Fe (5.9 keV), ^{57}Co (122 keV) and ^{60}Co (1333 keV) to cover various energy intervals.

4.2.3 Efficiency Calibration

The photopeak efficiency of the detector refers to the ratio of the actual events registered by the detector in each photopeak to the total number of events with a

defined energy emitted by the source of radiation. An accurate photopeak efficiency calibration of the system is necessary to quantify radionuclides present in the sample. It is essential that all settings and adjustment of the detector system be carried out prior to determining the efficiencies and this should be maintained until a new calibration is undertaken (IAEA, 1989)

In general, the efficiency of detection decreases logarithmically as a function of energy and it is geometric dependent. Appropriate radionuclides must be selected for use as standards in efficiency calibration. It is recommended to have a number of calibration points approximately between 60 keV and 2000 keV (IAEA, 1989).

The efficiency calibration curve was made using different energy peaks covering the range up to 2000 keV. Measurements were performed with the calibration standard. The efficiency calibration was performed by acquiring a spectrum of the calibration standard until the count rate at the peak of total absorption can be calculated with statistical uncertainty of less than 1% at a confidence level of 95%.

The net count rate was determined at the photopeaks for all the energies to be used for the determination of the efficiency of the calibration standard at the time of measurement. The efficiency at each energy was plotted as a function of the peak energy and extrapolated to determine the efficiencies at other peak energies for each of the measurement geometrics.

To calculate the absolute efficiency, the following equation (Cember and Johnson, 2009) was used

$$\varepsilon(E_\gamma) = \frac{N}{A*P*t} \qquad \text{(Eq. 4.2)}$$

where N is the full energy peak net count corresponding to the gamma photons with energy E_γ and gamma emission probability P, A is the activity of the source and t is the counting time.

The absolute efficiency of the detector was calculated at the specific energy of the standard sources for the same geometry of the samples. The absolute efficiency was calculated at any gamma energy of interest in the energy range below 2000 keV, using

the following equation:

$$\ln \varepsilon(E_\gamma) = a_o + a_1(\ln E_\gamma)^1 + a_2(\ln E_\gamma)^2 \qquad \text{(Eq. 4.3)}$$

where a_o, a_1, a_2 are calibration constants for a given geometry and the other symbols have the usual meaning given earlier in the passage. The efficiency calibration curve is shown in Figure 4.3.

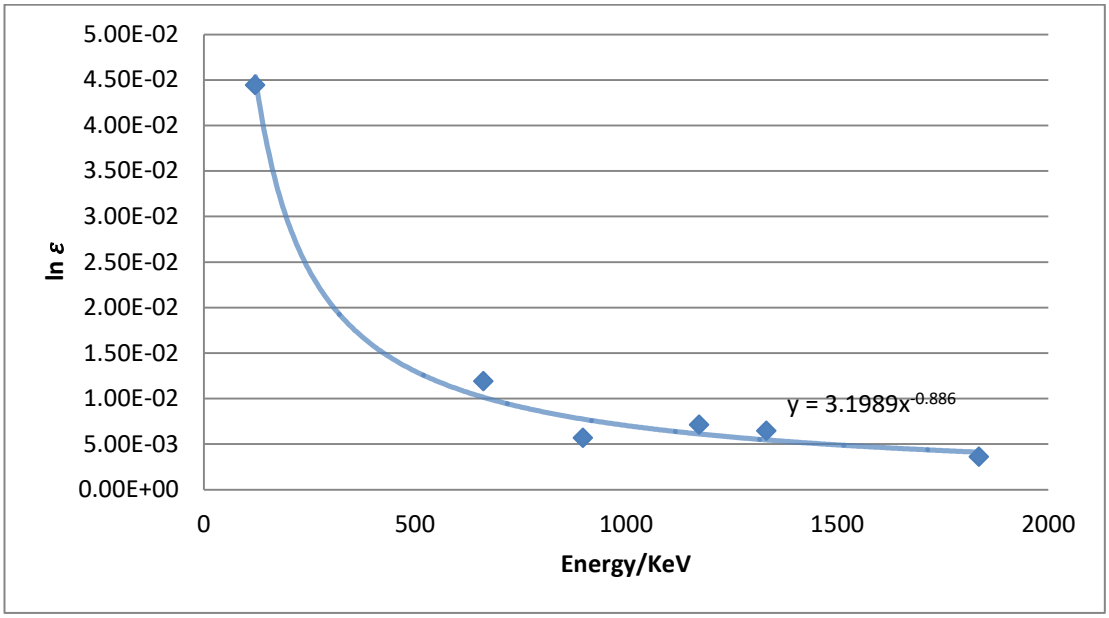

Figure 4.3**:** Efficiency calibration Curve

From the efficiency calibration curve, the following expression was obtained:

$$\ln \varepsilon = 0.4853 - 0.6616 \ln E_{\gamma} \qquad \text{for } E_{\gamma} > 100 \text{ keV} \qquad \text{(Eq.4.4)}$$

4.2.4 Determination of Minimum Detectable Activity

Minimum detectable activity (MDA) is defined as the smallest quantity of radioactivity that could be measured under specified conditions. The MDA is an important concept in low level counting particularly in environmental level systems where the count rate of a sample is almost the same as the count rate of the background. Under these conditions, the background is counted with a blank, such as sample holder, and everything else that may be counted with an actual sample. The minimum detectable activities (MDA) were calculated from the background spectrum for gamma measurements according to equation (4.5) (Hartwell, 1975)

$$\text{MDA} = \frac{\left(2.71 + 4.65\sqrt{N_{TB}\left(\frac{t_T}{t_B}\right) + N_C}\right)}{t_T . I . \varepsilon} \qquad \text{(Eq.4.5)}$$

Where;

N_{TB} is the background count for the region of interest of each radionuclide

t_T is the sample measurement time

t_B is the background counting time,

N_C is the integral

I is the gamma emission probability (gamma yield) of each radionuclide,

ε is the photopeak efficiency for the measured gamma ray energy.

4.3 Calculation of Specific Activity

Calculations of count rates for each detected photopeak and concentrations (activity per unit mass or specific activity) of detected radionuclides depend on the establishment of secular equilibrium in the samples. The ^{232}Th concentration was

determined from the average concentrations of ^{212}Pb (238.6 keV) and ^{228}Ac (911.1 keV) in the samples and that of ^{226}Ra was determined from the average concentrations of the ^{214}Pb (351.9 keV) and ^{214}Bi (609.3 and 1764.5 keV) decay products.

The activity concentration in Bq kg^{-1} (A) in the beach sand samples were calculated as follows:

$$A = \frac{N_p}{P * \varepsilon * m} \qquad \text{(Eq. 4.6)}$$

where N_p = the (cps) sample – (cps) BG, P is the abundance of the gamma line in a radionuclide, ε is the measured efficiency for each gamma line observed for the same number of channels either for the sample or for the calibration source and m the mass of the sample in kilograms.

4.4 Estimation of Doses

4.4.1 Estimation of Absorbed Dose Rate

The outdoor air-absorbed dose rates due to terrestrial gamma rays at 1m above the ground level was calculated from ^{226}Ra, ^{232}Th and ^{40}K concentration values in sand assuming that the other radionuclides, such as ^{137}Cs, ^{90}Sr and the ^{235}U decay series can be ignored as their contributions are expected to be negligible to the total dose from environmental background.

The absorbed dose rate at 1 m above the ground (in nGy h^{-1}) due to Ra, Th and K was calculated respectively, using the following equation.

$$D(nGyh^{-1}) = 0.0417\ A_K + 0.462\ A_{Ra} + 0.604 A_{Th} \qquad \text{(Eq. 4.7)}$$

where A_K, A_{Ra} and A_{Th} (Bq/kg) are the mean activity of ^{40}K, ^{226}Ra and ^{232}Th. The corresponding dose conversion coefficients transform the specific activities into absorbed dose rate. In the current work, the considered dose rate conversion factors for ^{238}U, ^{232}Th and ^{40}K were used in all subsequent dose rate calculations are those determined by Saito et al. (1990). These conversion factors have been used previously for related calculations in the UNSCEAR (1993) report. The dose conversion factors used in the calculation for ^{226}Ra, ^{232}Th and ^{40}K were 0.462, 0.604 and 0.0417, respectively.

In the above conversion factors, it is assumed that all the decay products of ^{226}Ra and ^{232}Th are in radioactive equilibrium. The published maximal admissible (permissible) dose rate is 55 nGy/h.

4.4.2 Estimation of Annual Effective Dose Equivalent

The absorbed dose rate in air at 1 metre above the ground surface does not directly provide the radiological risk to which an individual is exposed (Jibiri et al. 2007). The absorbed dose can be considered in terms of the annual effective dose equivalent from terrestrial gamma radiation which is converted from the absorbed dose by taking into account three factors, namely the conversion coefficient from absorbed dose in air to effective dose, the indoor occupancy factor and the outdoor occupancy factor. The annual effective dose equivalent (AEDE) can be estimated using the following formula (UNSCEAR 2000):

For indoor:

$$AEDE = D\ (nGyh^{-1}) * 8760h * 0.8 * 0.7\ Sv\ Gy^{-1} \qquad \text{(Eq.4.8)}$$

For Outdoor:

$$AEDE = D\ (nGyh^{-1}) * 8760h * 0.2 * 0.7\ Sv\ Gy^{-1} \qquad \text{(Eq. 4.9)}$$

Where 0.8 and 0.2 are the occupancy factors for indoor and outdoor respectively and 8760 is the total time of the year in hours. 0.7 Sv h^{-1} is the conversion factor for external gamma radiation.

4.5 Calculation of Hazard Indexes

4.5.1 Radium Equivalent Activity (Ra_{eq})

Radium equivalent activity (Ra_{eq}) is used to assess the hazards associated with materials that contain $^{238}U(^{226}Ra)$, ^{232}Th and ^{40}K in Bq/kg, which is, determined by assuming that 370 Bq/kg of ^{226}Ra or 260 Bq/kg of ^{232}Th or 4810 Bq/kg of ^{40}K produce the same γ dose rate (Beck, 1972).

Radium equivalent activity indices were calculated using the relation (Beck, 1972 and Chang et al. 2008).

$$Ra_{eq} = A_{Ra} + 1.43\ A_{Th} + 0.077\ A_K \qquad \text{(Eq. 4.10)}$$

Where the constants represent conversion factors (nGy h^{-1} *per* Bq kg^{-1}) calculated by the Monte Carlo technique for radionuclides and A_{Ra}, A_{Th} and A_K are the specific activities of ^{226}Ra, ^{232}Th and ^{40}K in Bq kg^{-1} respectively.

4.5.2 External Hazard Index (H_{ex})

The external hazard index is an evaluation of the hazard of the natural gamma radiation. The prime objective of this index is to limit the radiation dose so that annual dose equivalent limit of $1mSvy^{-1}$ is not exceeded. In order to evaluate this index, a model proposed by Beretka and Mathew (1985) was used in the current study.

The external hazard indices were calculated using the equation (Chang et al. 2008)

$$H_{ex} = \frac{A_{Ra}}{370} + \frac{A_{Th}}{295} + \frac{A_K}{4810} \qquad \text{(Eq. 4.11)}$$

Here, it is assumed that the same dose rate is produced from 370 Bq kg^{-1} ^{226}Ra or 259 Bq kg^{-1} ^{232}Th or 4810 Bq kg^{-1} ^{40}K present in the same matrix.

This model did not take into consideration the wall thickness, and the existence of doors and windows.

4.5.3 Internal Hazard Index (H_{in})

The internal hazard index should be less than unity for the radiation hazard to be considered negligible. Inhalation of alpha particles emitted from the short-lived radionuclides radon (^{222}Rn, the daughter product of ^{226}Ra) and thoron (^{220}Rn, the daughter product of ^{224}Ra) are also hazardous to the respiratory tract. This hazard can be quantified by the internal hazard index (H_{in})

The internal hazard indices were calculated using the equation (Chang et al. 2008)

$$H_{in} = \frac{A_{Ra}}{159} + \frac{A_{Th}}{295} + \frac{A_K}{4810} \qquad \text{(Eq. 4.12)}$$

The maximum permissible concentration for radium is therefore reduced to half the normal limit (Chang et al. 2008)

4.5.4 Excess Lifetime Cancer Risk (ELCR)

Excess Lifetime Cancer Risk, gives the probability of developing cancer over a lifetime at a given exposure level, considering 70 years as the Life Expectancy. It was calculated using the following equation (Taskin, et. al., 2009):

$$ELCR = AEDE \times DL \times RF \qquad (Eq.\ 4.13)$$

Where AEDE is the Annual Effective Dose Equivalent, DL is the average Duration of Life (estimated to be 70 years) and RF is the Risk Factor ($10^{-3}Sv^{-1}$) i.e. fatal cancer risk per Sievert. For stochastic effects, ICRP 103 uses values RF as 0.05 Sv^{-1} for the public.

4.6 Multivariate Statistical Analysis of the Data

Multivariate exploratory data analysis involves the application of both supervised and unsupervised pattern recognition techniques to detect and explore the distribution of radionuclide types and activity levels in relation to the other radiological parameters of the samples. Unsupervised techniques were used for clustering with respect to radionuclide activity concentrations and radiological parameters as well as site classification. Mean centred data sets were used in the analyses. The samples were characterized by their gamma-ray spectral data or activity concentrations and radiological parameters. The data was arranged in the form of matrices with the samples as rows and variables as columns.

Sediment data were subjected to PCA analysis. The data matrices were column centred by subtracting the mean value of each column from each of the 12

individual elements followed by column standardization of individual variables. This was done by subtracting the mean of column elements from individual elements and then dividing by individual column standard deviation. These were then subjected to PCA to give a visualization of the data structure in the form of 2D plots of residual variances, variances against PCs, rotated scores for PCs, and rotated loadings for PCs.

Mean, maxima, minima, standard deviation, skewness, kurtosis, correlation analyses, PCA and CA were done using SPSS v.20 software package.

CHAPTER 5

RESULTS AND DISCUSSION

Field observations and measurements, gamma-ray spectrometry, data analyses and results of the thesis research are presented and discussed in this Chapter. The concentrations of natural radionuclides (^{238}U, ^{232}Th and ^{40}K), determined by using HPGe detector, in sand from the selected beaches were calculated. The values of the mean specific activities of the natural radionuclides, the terrestrial absorbed dose rate, the mean radium equivalent, external and internal hazard index as well as the effective doses from external exposures were calculated, with the aim of evaluating the environmental natural radioactivity and radiological health hazard for the area under study. Radioactivity diversity within the Costal Belt of Ghana, its classification, and relationships between sampled beaches are presented and discussed with the aid of multivariate statistical data analysis.

5.1 Secular Equilibrium in Beach Sand Samples

Natural disturbance, sample collection and preparation may all cause disequilibrium in beach sand samples; therefore the prepared samples were sealed and stored in Marinelli beakers for one month to allow for secular equilibrium. To avoid any wrong estimation of ^{238}U (^{226}Ra) and ^{232}Th due to radon escape from the sand samples, this study also measured whether the radioactive equilibrium of radium precursors and their radon progeny and associated decay products had been established in the sand samples. The sands sampled from the Volta Region were used to investigate radioactive equilibrium.

With regard to radon loss, ^{222}Rn which has a 3.8 day half-life should take approximately 27 days to reach equilibrium with its parent (^{226}Ra) in the uranium chain while ^{220}Rn has only a 55.6 second half-life and would rapidly grow into its parent (^{224}Ra) in the thorium chain. Any radon loss would underestimate the interpreted ^{226}Ra content. As such, in the present study, the samples were sealed with PVC tape. In-growth of the short-lived progeny ^{212}Pb (238 keV and 300 keV), ^{208}Tl (583 keV) in the thorium chain and ^{214}Pb (295 keV and 351 keV) and ^{214}Bi (609 keV) in the uranium chain, from the first to eighth day and over periods of 12, 22 and 33 days after sample preparation. The small differences in the activity of each growth curve as a function of time may result from accumulation of bismuth and lead in natural sand samples leading to rapid approach to activity equilibrium with the respective parents. In addition, it might be expected that the only appreciable radon loss would be from the surfaces of a sand sample, the bulk being retained within the body of the sample. Comparison of the activity of ^{212}Pb and ^{212}Bi from the thorium chain and ^{214}Pb and ^{214}Bi in the uranium chain, 33 days after sample preparation, indicates that the radioactive equilibrium was maintained and that there was no significant, measureable loss of any the decay products during sample storage. The decay progeny that follow ^{226}Ra and ^{224}Ra in the decay chains would therefore also achieve this equilibrium. It can be noted that although it would take about 27 days for ^{222}Rn to achieve equilibrium with its parent, only ^{222}Rn decay products were measured and thus radioactive equilibrium can be approached in about 2 hours under normal circumstances. As the longest half-life of radionuclides prior to ^{210}Pb in the uranium chain is ^{214}Pb which has a half-life of 26.8 minutes, radioactive equilibrium was achieved in a short period of time, of the order of a few hours. The presence of ^{210}Pb ($t_{1/2}$ = 22 years) resulting in the further growth is

relatively slow and difficult to observe. In the thorium decay chain, there are no long-lived radionuclides after ^{220}Rn. Therefore, reaching equilibrium of ^{220}Rn and its decay products only influenced by the time required for the build-up of ^{212}Pb ($t_{1/2}$ =10.6 hours).

Since the activity of each radionuclide in the chain should be the same if radioactive equilibrium is achieved, the activity ratio of ^{226}Ra with its decay products and between its daughters can be used as an indicator for the radioactive equilibrium. From Figure 5.1 and 5.2, it can be seen that the R-squared values, for ^{226}Ra/^{214}Pb and ^{214}Pb/^{214}Bi activity plots are all close to unity. This means that the activity values of ^{226}Ra, ^{214}Pb, and ^{214}Bi are similar and the assumption of radioactive equilibrium being established in the studied sand samples is valid.

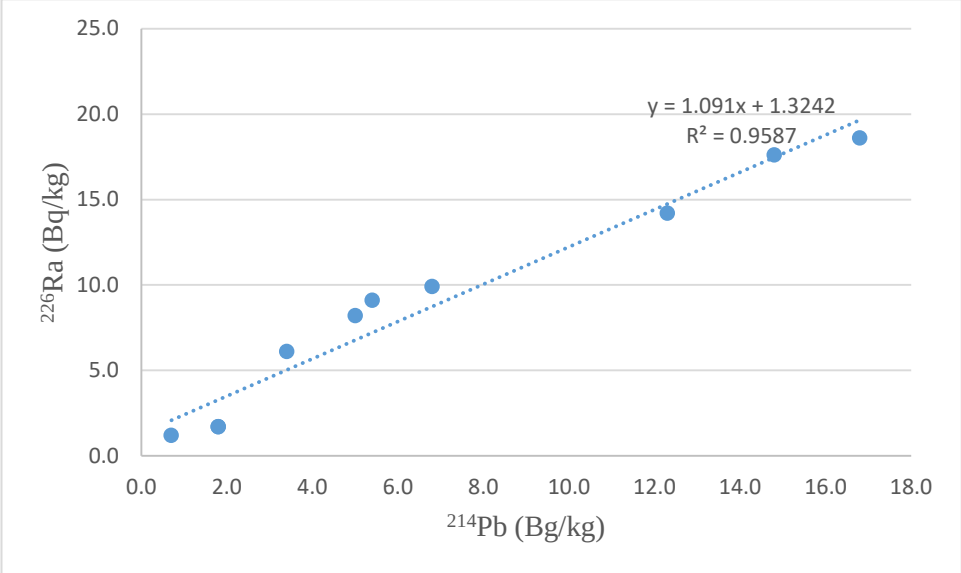

Figure 5.1: Relation between ^{226}Ra and ^{214}Pb

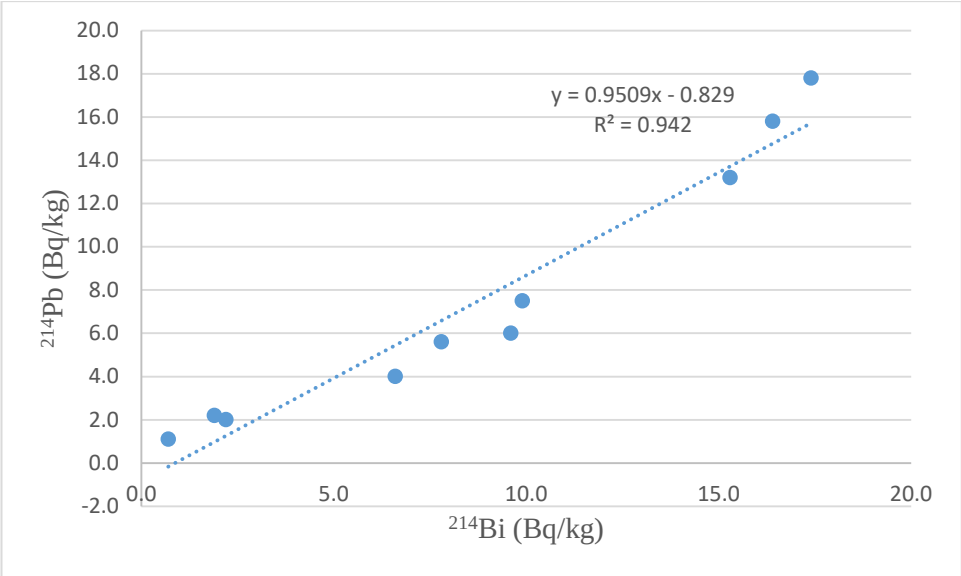

Figure 5.2: Relation between ^{214}Pb and ^{214}Bi

5.2 Specific Activities of Natural Radionuclides in Samples

Determination of activity concentrations requires knowledge of specific correction factors including, a self-attenuation corrections, decay- and life-time corrections and coincidence corrections. These have been applied to the analysis where appropriate. With only a small difference in the density between the reference sources and sand samples, the self -attenuation correction factor was not taken into account in this study. The weighted means for the activity was also applied in order to achieve the best estimate of the activity concentrations for given chains. The use of independent measurements of multiple, discrete gamma-ray lines from the same decay chains allows a significant reduction in the statistical uncertainty of the derived activity concentrations compared to the use of a single transition.

Specific Activities due to the presence of ^{238}U, ^{232}Th and ^{40}K radionuclides have been determined in all the collected sand samples. The values of the mean Specific

Activities of the radionuclides in sand from the selected beaches are shown in Table 5.1a-e.

Table 5.1a: Mean Specific Activities of ^{238}U, ^{232}Th and ^{40}K in beach sand from the Volta Region.

Town	**A_{sp}(BqKg^{-1})**		
	^{238}U	**^{232}Th**	**^{40}K**
Aflao	16.26	18.99	104.90
Denu	10.57	24.81	103.90
Kedzi	1.87	3.84	124.30
Keta	6.87	15.33	147.40
Tegbi	2.26	6.01	164.00
Woe	6.84	11.43	127.50
Anloga	14.33	16.63	139.80
Whuti	2.42	7.26	117.40
Dzita	9.45	18.14	150.40
Atiteti	17.53	20.74	105.90

Table 5.1b: Mean Specific Activities of ^{238}U, ^{232}Th and ^{40}K in beach sand from the Greater Accra Region.

Town	**A_{sp}(BqKg^{-1})**		
	^{238}U	**^{232}Th**	**^{40}K**
Ada Foah	7.60	5.40	51.00
Old Ningo	16.50	26.90	175.60
New Ningo	13.50	20.50	128.90
Prampram	2.50	2.50	51.40
Kpone	8.10	5.80	71.40
Tema	11.80	16.10	227.50
Nungua	7.50	6.40	71.60
Teshie	9.30	9.60	47.80
Labadi	5.90	6.90	62.40
Bortianor	6.60	5.40	67.90

Table 5.1c: Mean Specific Activities of ^{238}U, ^{232}Th and ^{40}K in beach sand from the Central Region.

Town	$A_{sp}(BqKg^{-1})$		
	^{238}U	^{232}Th	^{40}K
Gomoah Fetteh	2.2	5.2	92.00
Senya Breku	4.2	8.5	97.60
Winneba	2.2	4.0	93.80
Apam	4.5	12.6	95.80
Mumford	3.0	5.5	101.10
Saltpond	5.8	11.6	97.70
Anomabo	2.3	4.7	103.00
Biriwa	5.5	12.5	92.60
Moree	27.0	13.2	276.00
Elmina	20.1	11.2	229.00
Komenda	2.5	5.7	51.40

Table 5.1d: Mean Specific Activities of ^{238}U, ^{232}Th and ^{40}K in beach sand from the Western Region.

Town	$A_{sp}(BqKg^{-1})$		
	^{238}U	^{232}Th	^{40}K
Shama	8.3	5.8	71.40
Sekondi	9.4	15.9	128.00
Takoradi	9.1	15.2	84.40
Dixcove	7.5	6.5	67.10
Axim	9.3	10.0	71.60
Esiama	5.3	4.2	47.80
Eikwe	5.6	6.9	62.40
Atuabo	6.2	5.3	51.00
Half Assini	5.1	7.1	49.80
New Town	5.8	8.2	50.70

Table 5.1e: Statistics of Specific Activities of ^{238}U, ^{232}Th and ^{40}K in beach sand from the Study Area.

Statistics	$A_{sp}(BqKg^{-1})$		
	^{238}U	^{232}Th	^{40}K
Minimum	1.87	2.50	47.80
Maximum	27.00	26.90	276.00
Mean	8.01	10.44	103.79
Standard Deviation	5.48	6.14	52.76

The content of ^{238}U ranges from 1.87 to 27.00 Bq kg^{-1}, ^{232}Th content ranges from 2.50 to 26.90 Bq $kg^{-1}$and ^{40}K content ranges from 47.80 to 276 Bq kg^{-1}. The mean specific activities for the regions are as shown in Table 5.2.

Table 5.2: Mean Specific Activities of ^{238}U, ^{232}Th and ^{40}K in sand from the Regions

Region	$A_{sp}(BqKg^{-1})$		
	^{238}U	^{232}Th	^{40}K
Volta	8.842	14.317	128.550
Great Accra	8.930	10.550	95.550
Central	7.195	8.615	120.909
Western	7.143	8.480	68.420

The natural radionuclide contents in soil from UNSCEAR 2000 show the mean specific activity in Egypt for ^{238}U, ^{232}Th and ^{40}K to be 17, 18 and 320 Bq kg^{-1} respectively. The average activity concentrations determined in the sand samples are lower than the published worldwide average activity concentration of 33 Bq$kg^{-1}$for ^{238}U, 32 Bq.kg^{-1} for ^{226}Ra, 45 Bq.$kg^{-1}$for ^{232}Th and 412 Bq.kg^{-1} for ^{40}K (UNSCEAR 2008). The concentrations of natural radionuclides in various types of sand from

different parts of the world, are also provided and compared with the data obtained in the present work in Table 5.3

Table 5.3: Comparison of Specific Activities of ^{232}Th, ^{226}Ra and ^{40}K (Bq kg^{-1}) in sand samples from Greater Accra Region and other studies in different beaches of the world. Modified from UNSCEAR 2000

Location	**A_{sp}(BqKg^{-1})**		
	^{238}U	**^{232}Th**	**^{40}K**
Beach Sand, Ghana	1.87-27.0	2.5-26.9	47.8-276.0
Ganet Safaga	184	201	877
Masab El-Ghazel	174	185	759
Preta beach Southeastern Brazil	128-349	54-180	47-283
Dois Rios beach, Southeastern Brazil	12-87	6-78	269-527
Visakhapatnam, India	300-600	100-400	-
Northeast Coast, Spain	5-44	5-19	136-1087
Ullal, India	1842	374	158
Kalpakkam, India	352-3872	36-258	324-405
Red seashore sediment, Egypt	2.3-221.9	95.3-105.6	98-1011
Costal sand, Egypt	44.3-95.6	32.2-63.7	96-102
Beach sand, Al-Maidan, North Sinai,	146	108	77
Seabed sand, Tuen Mun Hong Kong	29.8	27.7	1210
Coastal Karnataka	489.6	249.2	55
Black sand, Brazil	25-2412	190-36620	-
Zircon, Bangladesh	1324	6439	472
Global average soil	10-50	7-50	100-700
	40	35	370
Global average soil	8–160	4–130	100 – 700
	32	45	420

Figure 5.3 gives the ratio of ^{232}Th/^{238}U for the 41 beach sand samples collected along the coast of Ghana. The ratio was found to lie in the range from 1.39 to 8.50 with the mean value of 4.31. The results show that the areas under investigation have uranium and thorium contents in the typical rock range with a ^{232}Th/^{238}U ratio

close to the continental crustal average concentration of 3.82, as reported by the NCRP (1987). Chiozzi et al. state that the agreement of these two values suggests that there is no significant fractionation during weathering or associated with the metasomatic activity in the monitored area.

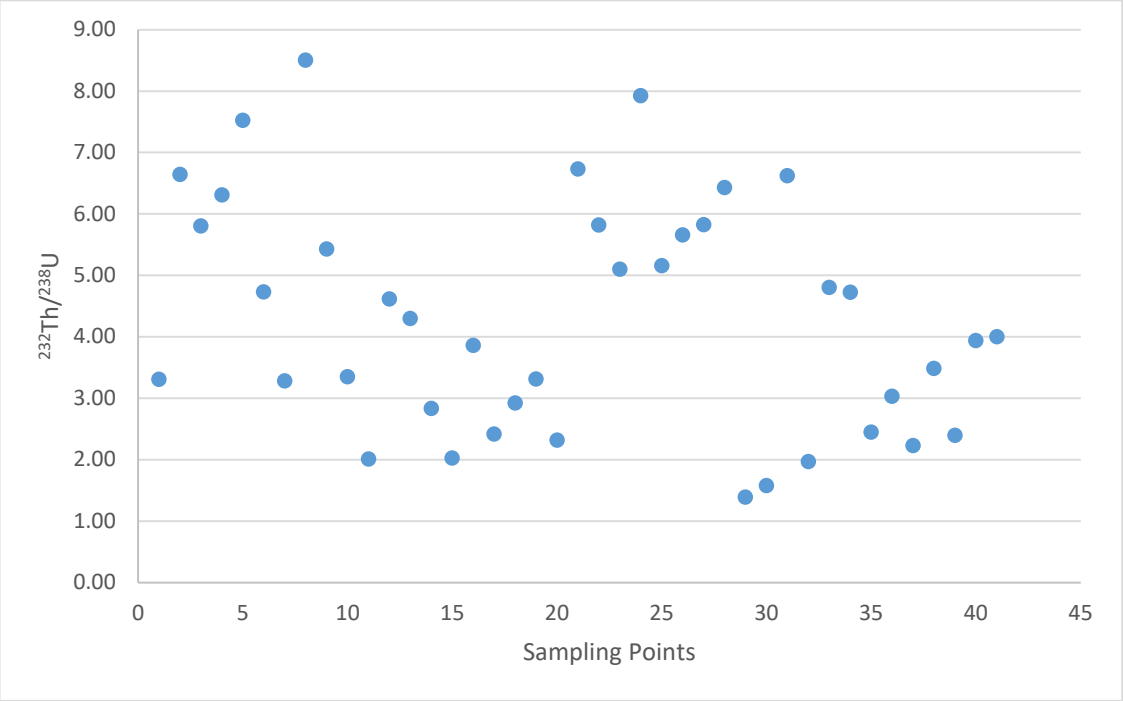

Figure 5.3: Ratio of $^{232}Th/^{238}U$ for the 41 beach sand samples

The correlation between ^{238}U and ^{232}Th concentrations in beach sand samples is shown in Figure 5.4. The solid line in the figure represents the best-fit between the ^{238}U and ^{232}Th concentrations is approximately a linear relationship with a correlation coefficient of 0.52.

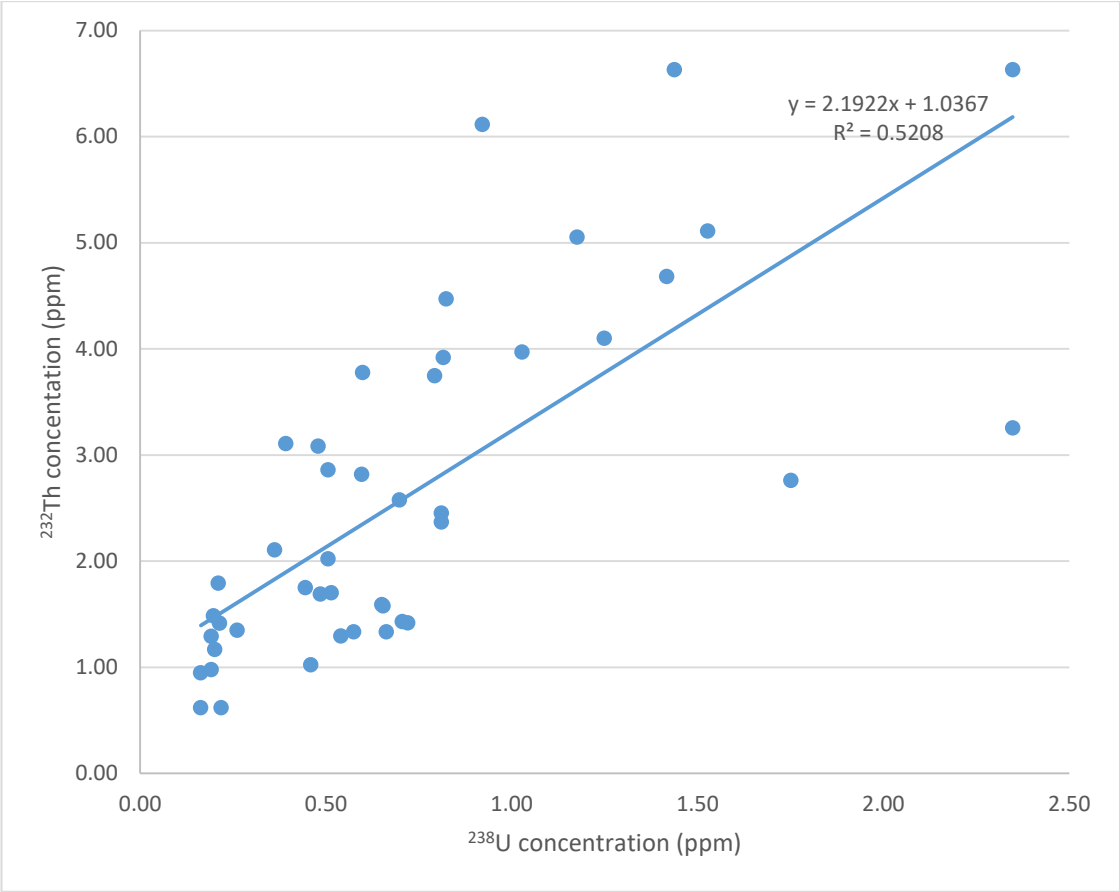

Figure 5.4: Correlation between ^{238}U and ^{232}Th concentrations in beach sand samples

5.3 Elemental Concentrations

Since the activity of the samples is also associated with the number of radioactive atoms in the samples, assuming ^{226}Ra in equilibrium with ^{238}U therefore the activity concentrations of ^{238}U, ^{232}Th and ^{40}K were then converted into the mass concentrations. Considering the fact that the primordial radionuclides (^{238}U, ^{232}Th, and ^{40}K) exhibit a constant atomic abundance in nature, it is possible to convert the specific activities of ^{238}U, ^{232}Th, and ^{40}K into massic elemental concentrations of U, Th, and K respectively in order to compare the different techniques using the following formula (Tzortzis et al., 2003)

$$C_E = \frac{T_{1/2} \cdot \mathrm{R} \cdot \mathrm{M_a}}{P_a \cdot \mathrm{N_A} \cdot ln2} \cdot A_{sp} \qquad Eq.(5.1)$$

where, C_E is the elemental concentration in sample, M_a is the atomic mass ($kgmol^{-1}$), $T_{1/2}$ is the half-life (seconds), P_a is the fractional atomic abundance in nature (%), N_A is Avogadro's constant (6.023×10^{23} $gmol^{-1}$), A_{sp} is the measured activity concentration ($Bqkg^{-1}$) of the radionuclide considered (^{238}U, ^{232}Th, or ^{40}K), and *R* is a constant with a value of 1,000,000 for U and Th (concentration in μgg^{-1}) or 100 for K (concentration in % of mass fraction).

The elemental concentrations of ^{238}U, ^{232}Th and ^{40}K were found to lie in the range of 0.16-2.35, 0.62-6.63 ppm, and 0.15-0.89% with the mean values of 0.70, 2.57 ppm, and 0.33% respectively (Table 5.4 a-e).

Table 5.4a: Elemental concentrations of ^{238}U, ^{232}Th and ^{40}K in beach sand from the Volta Region.

Town	Con(μg/g)%		
	^{238}U	^{238}U	^{238}U
Aflao	1.42±0.13	4.68±0.34	0.34±0.08
Denu	0.92±0.14	6.11±0.41	0.34±0.06
Kedzi	0.16±0.16	0.95±0.24	0.40±0.09
Keta	0.60±0.15	3.78±0.38	0.48±0.08
Tegbi	0.20±0.12	1.48±0.34	0.53±0.09
Woe	0.60±0.11	2.82±0.34	0.41±0.09
Anloga	1.25±0.14	4.10±0.42	0.45±0.08
Whuti	0.21±0.16	1.79±0.39	0.38±0.08
Dzita	0.82±0.15	4.47±0.32	0.49±0.09
Atiteti	1.53±0.11	5.11±0.35	0.34±0.10

Table 5.4*b*: Elemental concentrations of ^{238}U, ^{232}Th and ^{40}K in beach sand from the Greater Accra Region.

Town	Con(μg/g)%		
	^{238}U	^{232}Th	^{40}K
Ada Foah	0.66±0.14	1.33±0.46	0.16±0.07
Old Ningo	1.44±0.17	6.63±0.31	0.57±0.08
New Ningo	1.18±0.10	5.05±0.23	0.42±0.10
Prampram	0.22±0.17	0.62±0.45	0.17±0.08
Kpone	0.71±0.17	1.43±0.34	0.23±0.04
Tema	1.03±0.16	3.97±0.39	0.73±0.07
Nungua	0.65±0.14	1.58±0.36	0.23±0.08
Teshie	0.81±0.11	2.37±0.25	0.15±0.02
Labadi	0.51±0.10	1.70±0.41	0.20±0.03
Bortianor	0.58±0.15	1.33±0.24	0.22±0.03

Table 5.4c: Elemental concentrations of ^{238}U, ^{232}Th and ^{40}K in beach sand from the Central Region.

Town	Con(µg/g)%		
	^{238}U	^{232}Th	^{40}K
Gomoah Fetteh	0.19±0.09	1.29±0.35	0.30±0.02
Senya Breku	0.36±0.17	2.10±0.34	0.31±0.03
Winneba	0.19±0.17	0.98±0.32	0.30±0.03
Apam	0.39±0.17	3.11±0.37	0.31±0.03
Mumford	0.26±0.14	1.35±0.36	0.33±0.04
Saltpond	0.51±0.14	2.86±0.43	0.32±0.02
Anomabo	0.20±0.12	1.17±0.39	0.33±0.06
Biriwa	0.48±0.15	3.08±0.35	0.30±0.06
Moree	2.35±0.08	3.25±0.25	0.89±0.06
Elmina	1.75±0.13	2.76±0.41	0.74±0.05
Komenda	0.21±0.12	1.41±0.24	0.17±0.05

Table 5.4d: Elemental concentrations of ^{238}U, ^{232}Th and ^{40}K in beach sand from the Western Region.

Town	Con(µg/g)%		
	^{238}U	^{232}Th	^{40}K
Shama	0.72±0.12	1.42±0.35	0.23±0.06
Sekondi	0.82±0.15	3.92±0.34	0.41±0.06
Takoradi	0.79±0.14	3.75±0.32	0.27±0.05
Dixcove	0.65±0.11	1.59±0.37	0.22±0.06
Axim	0.81±0.12	2.45±0.36	0.23±0.07
Esiama	0.46±0.16	1.02±0.43	0.15±0.06
Eikwe	0.48±0.11	1.69±0.60	0.20±0.05
Atuabo	0.54±0.08	1.29±0.41	0.16±0.08
Half Assini	0.44±0.16	1.75±0.39	0.16±0.05
New Town	0.51±0.12	2.02±0.41	0.16±0.05

Table 5.4e: Statistics of Elemental concentrations of ^{238}U, ^{232}Th and ^{40}K in beach sand from the Study Area.

Statistics	Con(µg/g)%		
	^{238}U	^{232}Th	^{40}K
Minimum	0.16	0.62	0.15
Maximum	2.35	6.63	0.89
Mean	0.70	2.57	0.33

5.4 Terrestrial Absorbed Dose Rates Determined at the Selected Beaches

From the specific activity, it is possible to evaluate the dose rate (in nGy h^{-1}) due to terrestrial gamma rays only, at 1 m above the ground. External exposure to gamma rays from natural radioactive elements occurs outdoors and indoors. For evaluation of the annual dose, it is important to take into account the occupancy factor, i.e. how long people spend at a particular location and what they do while they are there. UNSCEAR 2000 report has proposed that the indoor occupancy factor is 0.8, implying that 20% of the day is spent outdoors, on average, around the world. The calculated absorbed gamma dose rate in air, due to the presence of the natural radionuclides in the sand are given in Table 5.5 a-d.

Table 5.5a: Absorbed Dose rates in air from ^{238}U, ^{232}Th and ^{40}K in beach sand from the Volta Region.

Town	Adsorbed Dose Rate(nGy/hr)
Aflao	23.35
Denu	24.20
Kedzi	8.37
Keta	18.58
Tegbi	11.52
Woe	15.38
Anloga	22.49
Whuti	10.40
Dzita	21.59
Atiteti	25.04

Table 5.5b: Absorbed Dose rates in air from ^{238}U, ^{232}Th and ^{40}K in beach sand from the Greater Accra Region.

Town	Adsorbed Dose Rate (nGy/hr)
Ada Foah	8.90
Old Ningo	31.19
New Ningo	23.99
Prampram	4.81
Kpone	10.22
Tema	24.66
Nungua	10.32
Teshie	12.09
Labadi	9.50
Bortianor	9.14

Table 5.5c: Absorbed Dose rates in air from ^{238}U, ^{232}Th and ^{40}K in beach sand from the Central Region.

Town	Adsorbed Dose Rate (nGy/hr)
Gomoah Fetteh	8.01
Senya Breku	11.14
Winneba	7.32
Apam	13.68
Mumford	8.90
Saltpond	13.76
Anomabo	8.22
Biriwa	13.95
Moree	31.93
Elmina	25.60
Komenda	6.74

Table 5.5d: Absorbed Dose rates in air from ^{238}U, ^{232}Th and ^{40}K in beach sand from the Western Region.

Town	Adsorbed Dose Rate (nGy/hr)
Shama	10.27
Sekondi	19.27
Takoradi	16.90
Dixcove	10.14
Axim	13.29
Esiama	6.93
Eikwe	9.31
Atuabo	8.16
Half Assini	8.72
New Town	9.75

5.5 Annual Effective Dose Equivalent

In all of the beaches investigated, the mean values of annual effective doses outdoor (Table 5.6) were lower than the worldwide average of 0.07 mSv y^{-1} published in UNSCEAR 2000. None of the beaches studied was considered a radiological hazard, because of the low values of gamma dose rates found in most of the samples investigated from the beaches. The annual external effective dose equivalents varied from 0.03 to 0.20 mSv y^{-1}, with an average value of 0.09mSv y^{-1}. In normal background areas, the average annual external effective dose from terrestrial radionuclides is 0.46 mSv y^{-1}. Therefore the annual external effective dose obtained for the beaches of Ghana is lower than the worldwide average normal background doses received from radionuclides of terrestrial origin. Figure 5.6 shows the average values of annual effective dose (mSv y^{-1}).

Table 5.6a: The annual external effective dose equivalent obtained for the beaches of the Volta Region.

Town	**AEDE (mSv y^{-1})**		
	Indoors	**Outdoors**	**Total**
Aflao	0.11	0.03	0.14
Denu	0.12	0.03	0.15
Kedzi	0.04	0.01	0.05
Keta	0.09	0.02	0.11
Tegbi	0.06	0.01	0.07
Woe	0.08	0.02	0.09
Anloga	0.11	0.03	0.14
Whuti	0.05	0.01	0.06
Dzita	0.11	0.03	0.13
Atiteti	0.12	0.03	0.15

Table 5.6b: The annual external effective dose equivalent obtained for the beaches of the Greater: Accra Region.

Town	AEDE (mSv y^{-1})		
	Indoors	**Outdoors**	**Total**
Ada Foah	0.04	0.01	0.05
Old Ningo	0.15	0.04	0.19
New Ningo	0.12	0.03	0.15
Prampram	0.02	0.01	0.03
Kpone	0.05	0.01	0.06
Tema	0.12	0.03	0.15
Nungua	0.05	0.01	0.06
Teshie	0.06	0.01	0.07
Labadi	0.05	0.01	0.06
Bortianor	0.04	0.01	0.06

Table 5.6c: The annual external effective dose equivalent obtained for the beaches of the Central Region.

Town	AEDE (mSv y^{-1})		
	Indoors	**Outdoors**	**Total**
Gomoah Fetteh	0.04	0.01	0.05
Senya Breku	0.05	0.01	0.07
Winneba	0.04	0.01	0.04
Apam	0.07	0.02	0.08
Mumford	0.04	0.01	0.05
Saltpond	0.07	0.02	0.08
Anomabo	0.04	0.01	0.05
Biriwa	0.07	0.02	0.09
Moree	0.16	0.04	0.20
Elmina	0.13	0.03	0.16
Komenda	0.03	0.01	0.04

Table 5.6d: The annual external effective dose equivalent obtained for the beaches of the Western Region.

Town	AEDE (mSv y^{-1})		
	Indoors	**Outdoors**	**Total**
Shama	0.05	0.01	0.06
Sekondi	0.09	0.02	0.12
Takoradi	0.08	0.02	0.10
Dixcove	0.05	0.01	0.06
Axim	0.07	0.02	0.08
Esiama	0.03	0.01	0.04
Eikwe	0.05	0.01	0.06
Atuabo	0.04	0.01	0.05
Half Assini	0.04	0.01	0.05
New Town	0.05	0.01	0.06

5.6 Radium Equivalent, External and Internal Hazard Indices

Since beach sands could be used as building materials, it is important to assess the gamma ray radiation hazards of sand to humans. The experimental results of Radium equivalent activity (Ra_{eq}) in Bq kg^{-1}, External hazard index (H_{ex}), and Internal hazard index (H_{in}) obtained are presented in Table 5.7 a-e.

Table 5.7a: Radium equivalent (R_{eq}), External hazard indices (H_{ex}) and Internal hazard indices (H_{in}) of the studied samples from the Volta Region.

Town	**R_{eq}**	**H_{ex}**	**H_{in}**
Aflao	51.49	0.14	0.18
Denu	54.04	0.15	0.17
Kedzi	16.94	0.05	0.05
Keta	40.14	0.11	0.13
Tegbi	23.49	0.06	0.07
Woe	33.01	0.09	0.11
Anloga	48.87	0.13	0.17
Whuti	21.84	0.06	0.07
Dzita	46.97	0.13	0.15
Atiteti	55.34	0.15	0.20

Table 5.7b: Radium equivalent (R_{eq}), External hazard indices (H_{ex}) and Internal hazard indices (H_{in}) of the studied samples from the Greater Accra Region.

Town	**R_{eq}**	**H_{ex}**	**H_{in}**
Ada Foah	19.25	0.05	0.07
Old Ningo	68.49	0.18	0.23
New Ningo	52.74	0.14	0.18
Prampram	10.03	0.03	0.03
Kpone	21.89	0.06	0.08
Tema	52.34	0.14	0.17
Nungua	22.17	0.06	0.08
Teshie	26.71	0.07	0.10
Labadi	20.57	0.06	0.07
Bortianor	19.55	0.05	0.07

Table 5.7c: Radium equivalent (R_{eq}), External hazard indices (H_{ex}) and Internal Hazard indices (H_{in}) of the studied samples from the Central Region.

Town	**R_{eq}**	**H_{ex}**	**H_{in}**
Gomoah Fetteh	16.77	0.05	0.05
Senya Breku	23.87	0.06	0.08
Winneba	15.09	0.04	0.05
Apam	29.89	0.08	0.09
Mumford	18.60	0.05	0.06
Saltpond	29.91	0.08	0.10
Anomabo	17.00	0.05	0.05
Biriwa	30.51	0.08	0.10
Moree	67.08	0.18	0.25
Elmina	53.75	0.15	0.20
Komenda	14.61	0.04	0.05

Table 5.7d: Radium equivalent (R_{eq}), External hazard indices (H_{ex}) and Internal hazard indices (H_{in}) of the studied samples from the Western Region.

Town	**R_{eq}**	**H_{ex}**	**H_{in}**
Shama	21.99	0.06	0.08
Sekondi	41.96	0.11	0.14
Takoradi	37.33	0.10	0.13
Dixcove	21.86	0.06	0.08
Axim	29.04	0.08	0.10
Esiama	14.88	0.04	0.05
Eikwe	20.17	0.05	0.07
Atuabo	17.63	0.05	0.06
Half Assini	19.09	0.05	0.07
New Town	21.43	0.06	0.07

Table 5.7e: Statistics of Radium equivalent (R_{eq}), External hazard indices (H_{ex}) and Internal hazard indices (H_{in}) of the studied samples.

Statistics	R_{eq}	H_{ex}	H_{in}
Minimum	10.03	0.03	0.03
Maximum	68.49	0.18	0.25
Mean	30.93	0.08	0.11
Standard Deviation	15.76	0.04	0.06

The values show that the maximum Ra_{eq} value obtained, 30.93 Bq kg^{-1}, for the studied area is lower than the internationally accepted reference value of 370 Bq kg^{-1}. The corresponding values for the external hazard and internal hazard indices are (0.18 and 0.25) respectively. All studied beaches, have, H_{ex} and H_{in} lower than the international accepted value of one (1).

5.7 Lifetime Cancer Risk

Table 5.8 shows Statistics of Excess Lifetime Cancer Risk of the studied areas. The Average and maximum excess lifetime cancer risk (ELCR) for all samples are lower than the world average of 1.45×10^{-3}(Taskin, et. al., 2009).

Table 5.8: Statistics of Excess Lifetime Cancer Risk of the studied samples.

Statistics	Excess Lifetime Cancer Risk x 10^{-3}		
	indoor	outdoor	total
Minimum	0.08	0.02	0.10
Maximum	0.55	0.14	0.69
Mean	0.25	0.06	0.31
Standard Deviation	0.12	0.03	0.15

A number of studies have been carried out worldwide for the determination of ELCR due to Gamma Radiation. A few of them have been given in Table 5.9. In some studies only the outdoor annual dose (E_{out}) has been accounted to evaluate the ELCR.

These studies include the determination of ELCR in and around Warri Refining and Petrochemical Company in Niger Delta, Nigeria, by Emelue et al. (2014). As per their report the risk of developing cancer is below the standard. In another study by Ramasamy et al. (2013), in high background radiation area, Kerala, India the average ELCR value calculated is 1.7×10^{-3}, which is six times higher than the world average for outdoors (0.29×10^{-3}). Taskin et al. (2009) reported the ELCR value as 0.50×10^{-3} in Kirklareli, Turkey. Ramasamy, et. al. (2009) carried out the evaluation of ELCR in river sediments of Karnataka and Tamilnadu, India. The average of ELCR was found to be 0.20×10^{-3} which is less than the world average.

Table 5.9: Comparison of Excess Lifetime Cancer Risk calculated during various studies

Study area	Medium	ELCR × 10^{-3}			Reference
		outdoor	indoor	total	
Niger Delta, Nigeria	Soil	Negligible	NA	Negligible	Emelue, Jibiri, & Eke, (2014)
Kerala, India	Soil	1.7	NA	1.7	Ramasamy, Sundarrajan, Paramasivam, Meenakshisundaram, & Suresh, (2013)
Kirklareli, Turkey	Soil	0.50	NA	0.50	Aytas et al., (2012)
Karnataka & Tamilnadu, India	Sediments	0.20	NA	0.20	Ramasamy et al., (2009)
Tulkarem Province-Palestine	Soil	0.17	0.78	0.95	Thabayneh & Jazzar, (2012)
Azad Kashmir, Pakistan	Soil	0.54	1.63	2.17	Rafique et al., (2014)
World Average		0.29		1.45	Taskin, et. al., (2009)
Coastal Ghana	Beach Sand	0.06	0.25	0.31	Present study

5.8 Statistical Analysis

Statistical behaviour of the measured data is presented in Table 4.8, which includes the range (minimum–maximum), arithmetic mean (AM), arithmetic standard deviation (SD), median, mode, skewness, kurtosis and the type of frequency distribution for the three radionuclides for all the sediment samples. The basic statistics show that the AM of activity concentrations are different from each other. Precipitation affects the natural radioactivity of sediments, when rain water mixes with SO_2 in the air, making the rain become acidic. Acid rain causes accelerated mobilization of many materials in sediments, especially ^{238}U (Sheppard & Sheppard, 1988).

Table 5.10: Descriptive statistics of radiological parameters

Variables	D_R	**AEDR**	R_{eq}	H_{ex}	H_{int}
Minimum	4.810	0.030	10.030	0.030	0.030
Maximum	31.930	0.200	68.490	0.180	0.250
Mean (AM)	14.335	0.087	30.935	0.084	0.105
Std. Deviation	7.214	0.045	15.763	0.042	0.056
Variance	52.035	0.002	248.460	0.002	0.003
Skewness	0.936	0.968	0.896	0.897	0.984
Kurtosis	-0.241	-0.161	-0.367	-0.459	0.008

The standard deviations, as shown in Table 5.10, are lower than the mean activity concentrations for each of the three radionuclides in all the samples; indicating non-uniformity in the distribution of the radionuclides in the samples.

5.8.1 Skewness

In Probability theory and Statistics, Skewness is a measure of the asymmetry of the probability distribution of a real valued random variable. Skewness has benefits in many areas. Many models assume normal distribution; i.e., data are symmetric about the mean. The normal distribution has a Skewness of zero. However, in reality, data points may not be perfectly symmetric. Therefore, an understanding of the Skewness of the dataset indicates whether deviations from the mean will be positive or negative. Skewness characterizes the degree of asymmetry of a distribution around its mean (Groeneveld & Meeden, 1984). Positive Skewness indicates a distribution with an asymmetric tail extending towards values that are more positive. Negative Skewness indicates a distribution with an asymmetric tail extending towards values that are more negative. Lower Skewness values form normal distributions. All the radionuclides concentrations in the samples have Positive Skewness values (Table 5.10) which indicates asymmetric distribution with the tail extending towards high concentrations.

5.8.2 Kurtosis

Kurtosis is a measure of the peakedness of the probability distribution of a real-valued random variable. It characterizes the relative peakedness or flatness of a distribution compared with the normal distribution. Positive Kurtosis indicates a relatively peaked distribution. Negative Kurtosis indicates a relatively flat distribution. Higher Kurtosis means more of the variance is the result of infrequent extreme deviations, as opposed to frequent modestly sized deviations. In the present case ^{238}U, ^{40}K and ^{232}Th have a negative Kurtosis which indicates relatively peaked distribution (Table 5.10).

5.8.3 Pearson's correlation coefficient analysis

Correlation analysis was carried out, as a bivariation statistics in order to determine the mutual relationships and strength of association between pairs of variables through calculation of the linear Pearson correlation coefficient. Results for Pearson correlation coefficients between all the studied radioactive variables for sediments are shown in Table 5.11.

Table 5.11: Pearson correlation coefficients between the studied radioactive variables for sand samples

	^{238}U	^{232}Th	^{40}K	D_R	AEDR	R_{eq}	H_{ex}	H_{in}
^{238}U	1							
^{232}Th	0.652**	1						
^{40}K	0.624**	0.480**	1					
D_R	0.876**	0.890**	0.771**	1				
AEDE	0.879**	0.882**	0.775**	0.998**	1			
R_{eq}	0.871**	0.908**	0.743**	0.999**	0.997**	1		
H_{ex}	0.871**	0.903**	0.745**	0.997**	0.995**	0.998**	1	
H_{in}	0.922**	0.868**	0.730**	0.992**	0.990**	0.992**	0.989**	1

**. Correlation is significant at the 0.01 level (2-tailed).

The high good positive correlation coefficient was observed between ^{232}Th and ^{238}U because uranium and thorium decay series occur together in nature (Tanaskovic, Golobocanin, and Miljevic, 2012). The U content is directly related to Th and K contents with high positive correlation coefficients of 0.652 and 0.624, respectively. In contrast, K and Th contents are proportional with a low positive coefficient of 0.480. Positive correlation coefficients were observed between ^{238}U, ^{232}Th and ^{40}K,

and all the radiological parameters. This implies a very strong relationship between the radionuclides in sediments and radiological parameters. Hence this strong relationship shows that all three radionuclides contribute to the emission of gamma radiation in all the locations.

5.8.4 Principal Components Analysis (PCA) Computation

A set of forty one (41) beach sand samples described by radionuclides and radiological parameters, namely; ^{238}U, ^{232}Th, ^{40}K, radium equivalent activity (R_{eq}), absorbed dose rate (D_R), annual effective dose rate (AEDR) and External hazard index (H_{ex}) were analysed in simultaneous manner with principal components analysis (PCA) method. As an input preparation for the principal components analysis, the sample data set was randomly arranged in a matrix **X** of 41 rows and 8 columns. The rows are the sand samples and the columns are the sand sample radionuclide parameters. The magnitudes of the values of radionuclide parameters are different in dimension. Differences in magnitude may distort the computation and the variables cannot obviously be analysed and compared. Standardization or normalization of the sample data matrix is required prior to undertaking the PCA. The sample data matrix $\mathbf{X_{41x8}}$ is randomly sampled and standardized by centring and scaling, by dividing each variable by its standard deviation, becoming $\hat{X}_{41x8}$.

The variance of a variable or the covariance between two variables, belong to the most important parameters in statistics, particularly in PCA method. The variance-covariance matrix $\mathbf{R}_{8X8}$ of the standardized matrix $\hat{X}_{41\times8}$ compiles the variances as diagonal elements and the covariances as off-diagonal elements. Once the data matrix is standardized, the variance-covariance matrix coincides with correlation

matrix. An alternative approach of computing the variance-covariance or correlation matrix with the standardized sample matrix is to determine the product of $\hat{X}^T\hat{X}$.

Table 5.12: Extraction Method: Extraction Sums of Squared Loadings

Component	Initial Eigenvalues			Extraction Sums of Squared Loadings		
	Total	% of Variance	Cumulative %	Total	% of Variance	Cumulative %
1	7.134	89.176	89.176	7.134	89.176	89.176
2	0.541	6.759	95.935			
3	0.316	3.954	99.888			
4	0.004	.054	99.943			
5	0.004	.045	99.988			
6	0.001	.012	100.000			
7	4.072E-6	5.090E-5	100.000			
8	5.585E-8	6.981E-7	100.000			

The results showed that there was only one eigen value higher than 1.000 and that this factor could explain over 89.176% of the total variance (Table 5.12). Normally, an ordination result was good if the value was 75% or better. As seen from Table 5.13, the first component (PC1) is loaded heavily (0.890 and 0.879, respectively) on uranium and thorium series. Fig. 5.5 shows the Scree plot of radionuclide activities and radiological parameters.

Table 5.13: Extraction Method: Principal Component Analysis.

Variables	Component
	1
^{238}U	0.890
^{232}Th	0.879
^{40}K	0.771
D_R	0.999
AEDR	0.998
R_{eq}	0.998
H_{ex}	0.997
H_{in}	0.995

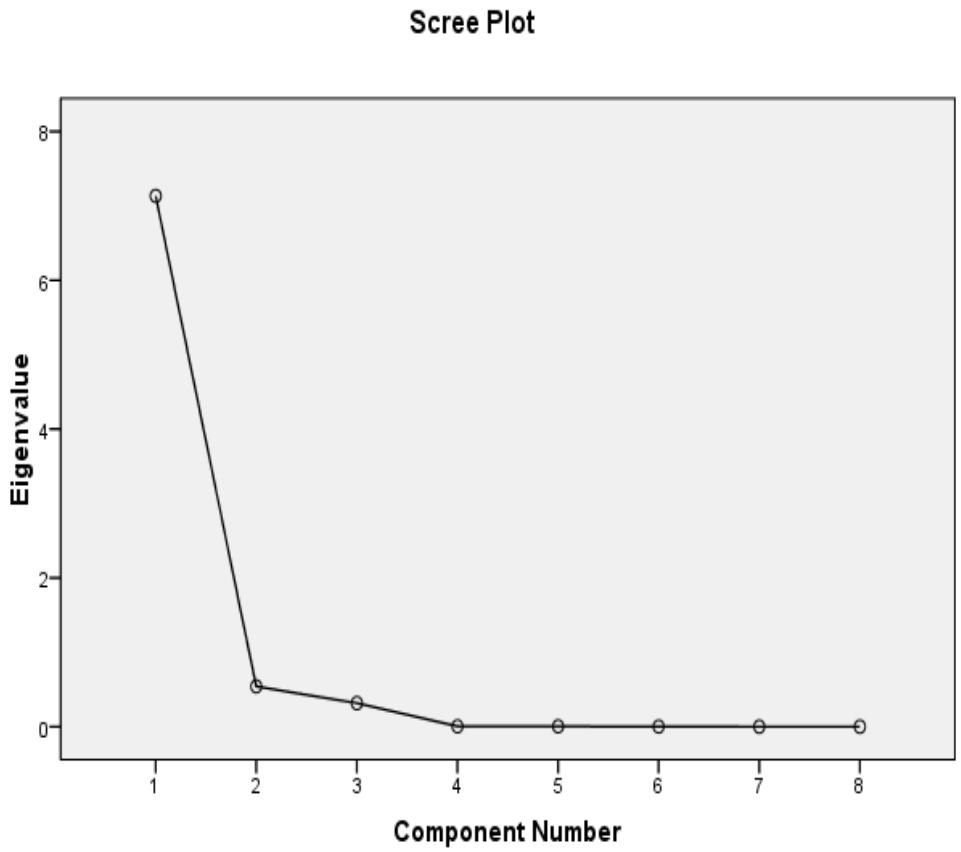

Figure 5.5: Scree plot of radionuclide activities and radiological parameters.

5.8.5 Cluster Analysis

In the PCA method, the interaction between the variables is investigated in detail. The columns of the sample matrix are under consideration. In cluster analysis, the samples are the main object of interest. Specifically, the distances between pairs of samples are calculated, compared and on the basis of the nearest similar distances a dendogram is built up. As in PCA, the original sample matrix should be standardized prior to calculating the distance.

The number of pair distances corresponding to all the combination of two samples out of n = 41 sand samples results in n(n-1)/2 = 820 distances. The computation of the differences between all possible pairs of samples results in a square symmetrical matrix D_{41X41} where each element is the distance of the two samples indicated by the corresponding column and row.

In Cluster Analysis, the average linkage method along with correlation coefficient distance was applied. The derived dendrogram is as shown in Figure 5.6. In this dendrogram, all eight (8) parameters were grouped into two statistically significant clusters. Cluster-I consists of ^{232}Th, ^{238}U and the radiological parameters, such as AEDE, H_{ex}, H_{in}, and D_R. Cluster-II consists of only ^{40}K. From this cluster analysis, ^{238}U and ^{232}Th contribute more to the radiological parameters than ^{40}K.

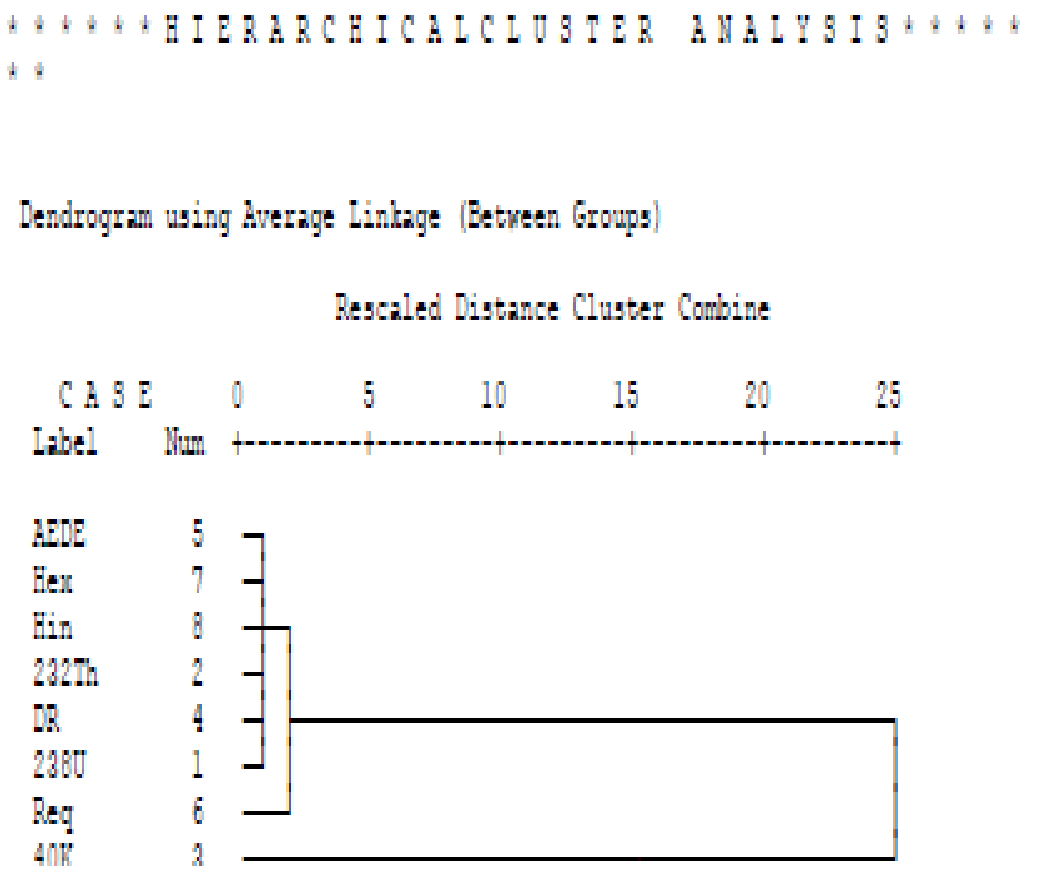

Figure 5.6**:** Dendrogram of radionuclide concentrations and radiological parameters matrix clustered by linkage method and sand groups associated with PCA biplot.

The samples with the highest similarities are arranged and placed into a hierarchy, then those pairs are merged and the matrix is recomputed. The process iterates until the dissimilarity matrix reaches the rank of two. The lower distance indicates that the sand samples are similar and a group or cluster is created. A certain group is more or less homogeneous in distances and distinct from the others. The constructed dendrogram is presented in the tree form as shown in Figure 5.7. The height of the tree between two samples or two groups of samples exhibit the distances between those samples or groups of sample. According to the dendrogram, the sand samples of similarity in distance are clustered into 5 groups. The sand samples, VR5, GR6 and CR9 are out of all groups.

The height of the dendrogram exhibits the similarities of distance between sand samples or groups of sand samples. At the height of 1, the sand samples are grouped into 8 clusters. The number of clusters is reduced to 3 when the height approaches 5 and at the height of 25, only one cluster exists. The maximum similarities detected among the sampling towns and the Spatial Groups identified on the basis of the dendogram are presented in Table 5.14.

From the cluster analysis, it can be concluded that the number of sampling towns can be reduced from the present 41 to 8 towns. The future eight monitoring towns can beVR-5, GR-8, CR-9 and any town from SG-1, SG-2, SG-3, SG-4, and SG-7.

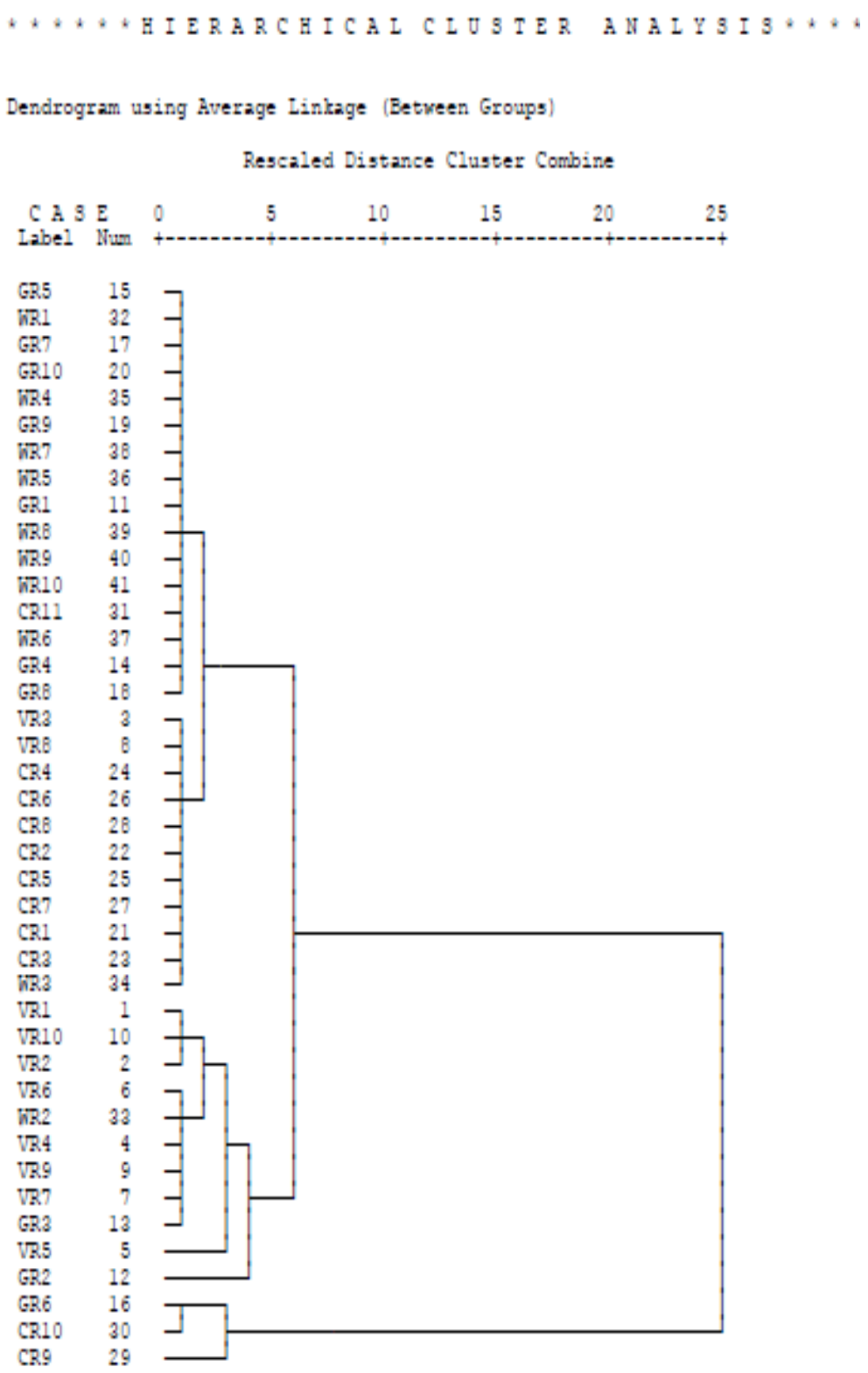

Figure 5.7**:** Dendrogram of sand sample matrix clustered by linkage method and sand groups associated with PCA biplot.

Table 5.14: Clustering strategy for development of Spatial Groups.

Sampling Towns	Spatial Groups
CR11	SG1
GR1	
GR4	
GR5	
GR7	
GR8	
GR9	
GR10	
WR1	
WR4	
WR5	
WR6	
WR7	
WR8	
WR9	
WR10	
CR1	SG2
CR2	
CR3	
CR4	
CR5	
CR6	
CR7	
CR8	
VR3	
VR8	
WR3	
VR1	SG3
VR2	
VR10	
GR3	SG4
VR4	
VR6	
VR7	
VR9	
WR2	
VR5	SG5
GR8	SG6
GR6	SG7
CR10	
CR9	SG8

CHAPTER 6

CONCLUSION AND RECOMMENDATIONS

This chapter presents the concluding remarks from the study. Recommendations have also been made to stakeholder institutions on the need for cost effective environmental monitoring based on the result of this study. The need for further studies has also been emphasized.

6.1 Conclusion

Radionuclide analysis and multivariate statistical classification of the beaches in Ghana have been carried out using HPGe based gamma-ray spectrometry data, PCA and HCA.

Specific Activities due to the presence of ^{238}U, ^{232}Th and ^{40}K radionuclides were determined in all the collected sand samples. The specific activity of ^{238}U ranges from 1.87 to 27.00 Bq kg^{-1}, ^{232}Th content ranges from 2.50 to 26.90 Bq $kg^{-1}$and ^{40}K content ranges from 47.80 to 276 Bq kg^{-1}. The activity values obtained in this study are comparable with published data of other works in Ghana indicating that the study areas have not been affected until now by any NORM activities that may have started in these environments.

The elemental concentrations of ^{238}U, ^{232}Th and ^{40}K were found to lie in the range of 0.16-2.35, 0.62-6.63 ppm, and 0.15-0.89% with the mean values of 0.70, 2.57 ppm, and 0.33% respectively.

The study shows that the average Ra_{eq} value, of 30.93 Bq kg^{-1}, for the studied area is lower than the internationally accepted value 370 Bq kg^{-1}. The corresponding values for the External Hazard (H_{ex}) and Internal Hazard indices (H_{in}) are (0.08 and 0.11) respectively. The values for H_{ex} and H_{in} are lower than the internationally accepted value of one (1.00).

The differences observed in the specific activities from the radionuclides ^{232}Th, ^{226}Ra and ^{40}K in relation to the sand profiles analysed, may be due to the different sand properties, like density, humidity and porosity, at each beach. The values of natural radioactivity and gamma absorbed dose rates estimated and hazard indices calculated show that the selected beaches have normal natural background radiation and beach sand from most of these beaches can be used in construction and may not pose any significant radiological hazard to users of these sands and beaches.

From the cluster analysis, it could be found that ^{238}U and ^{232}Th contribute more to the radiological parameters than ^{40}K and the number of sampling towns can be reduced from the present 41 to 8 towns.

The study offers a multivariate statistical environmental data reduction strategy for environmental monitoring. In this work, cluster analysis was used to evaluate spatial and temporal variations in beach sands. From the analysis, it was possible to develop an optimal sampling strategy, which could reduce the number of sampling stations, the number of samples collected and associate costs.

6.2 Recommendations

6.2.1 Regulatory and Environmental Protection Bodies

It is recommended to the regulatory and environmental protection bodies

- to design an optimal future sampling strategy which could reduce sampling frequency, number of sampling sites and associated sampling costs, Cluster Analysis should be considered.
- to improve on the prediction and classification of future measurements of samples other physical parameters such as, the size distribution, density, porosity, water retention and resistance to penetration of the sand grains should be included.

6.2.2 Research Institutions

The following areas are recommended for future research:

- Evaluation of natural radioactivity and radiological hazards in beach rocks along the shores of Ghana
- Multivariate Chemometric Analysis of Radon Concentration along the coast of Ghana.

REFERENCES

Agyepong, G.T., Yankson, P. W .K. and Ntiamoah-Baidu, Y. (1990). Coastal Zone Indicative Management Plan. Report prepared for the Environmental Protection Council. Accra, Ghana.

Ahmed, N.K. and El-Arabi, A.G.M. (2005). "Natural Radioactivity in Farm Soil and Phosphate Fertilizer and its Environmental Implications in Qena Governorate, Upper Egypt", Journal of Environmental Radioactivity 84: 51-64.

Alam M. N., Chowdhury M. I., Kamal M., Ghose S., Islam M. N., Mustafa M. N., Miah M. M. H., Ansary M. M. (1999). The ^{226}Ra, ^{232}Th and ^{40}K activities in beach sand minerals and beach soils of Cox's Bazar, Bangladesh. J. Environ. Radioact 46:243–250.

Al-Hamarneh, I.F. and Awadallah, M.I. (2009). "Soil Radioactivity Levels and Radiation Hazard Assessment in the Highlands of Northern Jordan", Radiation Measurements 44: 102-110.

Allersma, E. and Tilmans, W. M. K. (1993). Coastal conditions in West Africa: a review. Ocean and Coastal Management 19: 199-240.

Allisy, A. (1996), "Henri Becquerrel: The discovery of radioactivity", Becquerrel's Legacy: A Century of Radioactivity. Proceedings of a Conference, London: Nuclear Technology Publishing, 3-10.

Al-Sulaiti, H., Regan P. H., Bradley D. A., Malain D., et al. (2010). A preliminary report on the determination of natural radioactivity levels of the State of Qatar using high-resolution gamma ray spectrometry. Nuclear Instruments and Methods in Physics Research Section A: Accelerators, Spectrometers, Detectors and Associated Equipment. 619(1-3): 427-431.

Armah, A.K. (1991). Coastal erosion in Ghana; causes, patterns, research needs and possible solutions. Coastal Zone 91: 2463-2473.

Armah, A.K. and Amlalo, D. S. (1998). Coastal zone profile of Ghana. Gulf of Guinea Large Marine Ecosystems Project. Ministry of Environment, Science and Technology, Accra, Ghana.

Aytas, S. S. Yusan, S., Aslani, M.A., Karali, T.D., Turkozu, A., Gok, C., et al. (2012), Natural radioactivity of riverbank sediments of the Maritza and Tundja Rivers in Turkey, Journal of Environmental Science and Health, Part A, 47 pp. 2163–2172

Bannerman, P.O, Koranteng, K. A. and Yeboah, C. A. (2001). Ghana canoe frame survey, 2000. Information Report No. 33. Fisheries Department, Research and Utilisation Branch, Tema, Ghana.

Baulieu, F. (1989). A classification of presence/absence dissimilarity co-efficients. *Journal of Classification,* 6: 233–246

Beck, H.L. (1972). The physics of environmental radiation fields. Natural radiation environment II, CONF-720805 P2, Proceedings of the Second International Symposium on the Natural Radiation Environment.

Beretka, J., Mathew, P.J. (1985). Natural radioactivity of Australian building materials, industrial wastes and by-products. Health Phys. 48, 87–95.

Bikit, I., Slivka, J., Veskovic, M. Verga, E., Zikic-Todorovic, N., Mrda, D. and Forkapic, S. (2006). "Measurement of Danube Sediment Radioactivity in Serbia and Montenegro Using Gamma Ray Spectrometry", Radiation Measurements 41, 477-481.

Bolca, M., Sac, M.M., Cokuysal, B., Karali, T. and Ekdal, E. (2007). "Radioactivity in Soils and Various Foodstuffs from the Gediz River Basin of Turkey", Radiation Measurements 42: 263-270.

Bouwer, F. J. and Meklveen, J. W. (1978). 'Uranium Assay of Phosphate Fertilizers and Other Phosphatic Materials', Health Physics 34: pp. 345-352.

Burcham, W.E. (1973), Nuclear Physics: An Introduction (2nd edition), Harlow: Longman.

Carvalho, F.P., Oliveira, J.M., Lopes, I. and Batista, A. (2007). "Radionuclides from Past Uranium Mining in Rivers of Portugal", Journal of Environmental Radioactivity 98: 298-314.

Cember, H. and Johnson, T.E. (2009). Introduction to Health Physics (4^{th} edition), New York: McGraw-Hill Companies, Inc.

Cetnar, J. (2006). "General Solution of Bateman Equations for Nuclear Transmutations", Annals of Nuclear Energy 33: 640-645.

Chang, B.U., Koh, S.M., Kim, Y.J., Seo, J.S., Yoon, Y.Y., Row, J.W. and Lee, D.M. (2008). "Nationwide survey on the natural radionuclides in industrial raw minerals in South Korea", Journal of Environmental Radioactivity 99: 455-460.

Choppin, G. and Liljenzin, J. (2000). Radiochemistry and Nuclear Chemistry, 3^{rd} ed., USA, Butterworth-Heinemann, ISBN: 978-0-7506-7463-8.

Choppin, G., Liljenzin, J. and Rydberg, J. (2002). Radiochemistry and Nuclear Chemistry (3rd edition), USA: Butterworth-Heinemann.

Chowdhury, M.I., Alam, M.N. and Hazari, S.K.S. (1999). "Distribution of Radionuclides in the River Sediments and Coastal Soils of Chittagong, Bangladesh and Evalution of the Radiation Hazard", Applied Radiation and Isotope 51: 747-755.

Collier D.E. and Soldenhoff K.H. (2007). Deportment of NORM in the Processing of a Phosphate Ore Containing Rare Earths in Proceedings of an international symposium. Seville, Spain: International Atomic Energy Agency (IAEA), Vienna.

Curie, M., Debierne, A., Eve, A.S., Geiger, H., Hahn, O., Lind, S.C., Meyer, St., Rutherford, E. and Schweidler, E. (1931). "The Radioactive Constants as of 1930 Report of the International Radium-Standard Commission", Review of Modern Physics 3: 427- 445.

Davis, J. C. (2002). *Statistics and Data Analysis in Geology*. Third Edition, Johh Willey & Sons, New York

De Meijer R. J., James J. R., Jennings P. J., Koeyers J. E. (2001). Cluster analysis of radionuclide concentration in beach sand. Appl. Radiat. Isot 54:535–542.

Dei, L.A. (1972). The central coastal plains of Ghana: a morphological and sedimentological study. Z. F. Geolomorphological N.F. 16 (4): 415-431.

Directorate of Fisheries, (2003). Ghana: post-harvest fisheries overview. Directorate of Fisheries, Ministry of Food and Agriculture, Ghana. Brightsea Press Ltd, Exeter, UK.

El-Gamal, A., Nasr, S. and El-Taher, A. (2007). "Study of the Spatial Distribution of Natural Radioactivity in the Upper Egypt Nile River Sediments", Radiation Measurement 42: 457-465.

El-Kassas, I.A. (1991). A Geostatistical Study of Gamma Radioactivity at Some Anomalous Localities in Qatar Peninsula, The Arabian Gulf. J. King Saud University,. 4(Science (1)): 101-112.

Emelue H.U.. Jibiri, N.N. Eke B.C., (2014). Excess lifetime cancer risk due to gamma radiation in and around Warri refining and petrochemical company in Niger Delta Nigeria British Journal of Medicine & Medical Research, 4 (13), pp. 2590–2598

Faires, R.A. and Boswell, G.G.J. (1981). Radioisotope Laboratory Techniques (4th edition), London: Butterworth & Co (Publishers) Ltd.

Farmaki, G.E., Nikolaos, S.T., Simeonov, V. and Efstathiou, E.C. (2012) A Comparative Chemometric Study for Water Quality Expertise of the Athenian Water Reservoirs, Environ. Monit. Asses, 184:7635-7652.

Firestone, R. B. (1998). Table of Isotope, 8th ed., California, John Wiley & Sons Ltd., ISBN: 978-0471330561.

Freitas A. C., Alencar A. S. (2004). Gamma dose rates and distribution of natural radionuclides in sand beaches—Ilha Grande, Southeastern Brazil. J. Environ. Radioact 75: 211–223.

Friedlander, G. and Kennedy, J. W. (1986). Nuclear and Radiochemistry, 3rd ed., USA, John Wiley & Sons Ltd. ISBN: 0-471-86255-X.

Gardner-Lubbe, S., le Roux, N. J., and Gower, J. C. (2008). Measures of fit in principal component and canonical variate analyses. *Journal of Applied Statistics*, 35:947–965.

Gerhart, F., Kennedy, J.W., Macias, E.S. and Miller, J.M. (1981). Nuclear and radiochemistry. 3rd ed. New York: Jhon Wiley & Sons

Gilmore, G. (2008). Practical Gamma-ray Spectrometry, 2nd ed., England, John Wiley & Sons Ltd, ISBN: 978-0-470-86196-7.

Gonzalez, A. G. (2000). 'The Safety of Radioactive Waste Management: Achieving Internationally Acceptable Solutions', The IAEA Bulletin, vol. 42, no.3, 5-18.

Goraieb, K, Lopes, A.S., Sato, C.A., Segatelli, M.G., Silva, V.P., Verzoto, J.C., and Bueno, M.I.M.S. (2006). Characterization of Portland Cements by X-ray Spectrometry allied to Chemometrics, J. Chemometrics, 20: 455-463.

Gordon, A. (1999). *Classification, 2nd ed*. Cliapnian and Hall/ CRC Press.

Gordon, C. (1998). The state of the coastal and marine environment of Ghana. In: Ibe, C. and Zabi, S.G. (Eds.), State of the Coastal and Marine Environment of the Gulf of Guinea. UNIDO/UNDP/GEF CEDA.

Gower, J. (1985). Measures of similarity, dissimilarity and distance. In Kotz, S., Johnson, N.L. and Read, C.B. (Eds.). *Encyclopedia of Statistical Sciences*, 5: 397–405.

Hart, E. I. and Boag, J. W. (1962). Absorption spectrum of the hydrated electron in water and in aqueous solution. J. Am. Chem. Soc., 84: 4090-4095.

Harvey, B.G. (1969). Introduction to Nuclear Physics and Chemistry (2^{nd} edition), New Jersey: Prentice-Hall Inc.

Health, R.L. (1998). Gamma-Ray Spectrum Catalogue: Ge and Si Detector Spectra, 4th ed., Idaho National Engineering & Environmental Laboratory.

Henriksen, T. and Maillie, H.D. (2003). Radiation and HealthLondon and New York: Taylor and Francis Group.

Hsue, S. T., Langer, L. M., Tang, S. M. (1966). Precise Determination of the Shape of the Twice Forbidden Beta Spectrum of 137Cs. Nucl. Phys., 86: 47.

IAEA, (1989). Measurements of Radionuclides in Food and the Environment, in International Atomic Energy Agency Tech. IAEA: Vienna.

ICRP, (2007). The 2007 Recommendations of the International Commission on Radiological Protection. ICRP Publication 103. Ann. ICRP 37(2–4).

ICRP, (2009a). Application of the Commission's recommendations for the protection of people in emergency exposure situations. ICRP Publication 109. Ann. ICRP 39(1).

ICRP, (2009b). Application of the Commission's recommendations to the protection of people living in long-term contaminated areas after a nuclear accident or a radiation emergency. ICRP Publication 111. Ann. ICRP 39(3). ICRP 2013 Proceedings 187

International Commission on Radiological Protection (1991). "Radiation Protection", ICRP Publication 60. Elmsford, NY: Pergamon Press, Inc.

Jackson, D., Somers, K., and Harvey, H. (1989). Similarity coefficients: measures of co-occurrence and association or simply measures of occurrence. *The American Naturalist*, 133: 436–453.

Jibiri, N.N., Farai, I.P. and Alausa, S.K. (2007). "Estimation of Annual Effective Dose due to Natural Radioactive Elements in Ingestion of Foodstuffs in Tin Mining Area of Jos-Plateau, Nigeria", Journal of Environmental Radioactivity 94: 31-40.

Jolliffe, I. T. (2002). *Principal Component Analysis*. 2nd Ed. Springer-Verlag, New York, Inc.

Kannan V., Rajan M. P., Iyengar M. A. R., Ramesh R. (2002). Distribution of natural and anthropogenic radionuclides in soil and sand samples of Kalpakkam (India) using hyper pure germanium (HPGe) gamma ray spectrometry. Appl. Radiat. Isot. 57:109–119

Kessler, T., Hoffman, P., Greve, T., and Ortner, H.M. (2002) Optimization of the identification of chemical compounds by energy dispersive x-ray fluorescence spectrometry and subsequent multivariate analysis, X-ray Spectrom. 31: 383-390.

Khater, A. and Al-Sewaidan, H.A. (2008). "Radiation Exposure due to Agricultural Uses of Phosphate Fertilzers", Radiation Measurements 43: 1402-1407.

Klement, A.W. (1982). CRC Handbook of Environmental Radiation, Florida: CRC Press, Inc.

Knoll, G.F. (2000). Radiation Detection and Measurement, 3rd ed., New York, John Wiley & Sons Ltd., ISBN: 0-471-07338-5.

Krane, K. S. (1988). Introductory Nuclear Physics, Chichester: John Wiley & Sons Inc.

Kuma, H.A. (2004). General Overview of tourism. Paper presented at the Reduction of environmental impacts from coastal tourism stakeholders workshop, STEPRI 10 to 11th August 2004.

Kurnaz, A., Kucukomeroglu, B., Keser, R., Okumusoglu, N.T., Kprkmaz, F., Karahan, G. and Cevik, U. (2007). "Determination of Radioactivity Levels and Hazards of Soil and Sediment Samples in Firtina Valley (Rize, turkey)", Applied Radiation and Isotopes 65: 1281-1289.

Kurt, V. and Peter, F. (2008). Introduction to Multivariate Statistical Analysis in Chemometrics, CRC Press, New York.

L'Annunziata, M. F. (2007). Radioactivity: Introduction and History, Amsterdam: Elsevier B.V.

Laing, E. (1991). Ghana Environmental Action Plan (Vol. 1). E.P.C., Accra.

Lapp, R.E. and Andrews, H.L. (1972), Nuclear Radiation Physics (4th edition), London: Sir Isaac Pitman and Sons Ltd.

Leroy, C. and Rancoita, Pier-G., (2009). Principles of Radiation Interaction in Matter and Detection, 2nd ed., Singapore, World Scientific Publishing. ISBN-13: 978-981-281-828-7(pbk), ISBN-10: 981-281-828-6 (pbk).

Lilley, J. (2001). Nuclear Physics: Principles and Applications, Chichester: John Wiley & Sons, Ltd.

Mange, M. A., Maurer, H. F. W. (1992). Heavy Minerals in Colour. London: Chapman and Hall.

Martin, A. and Harbison, S. (2006). An Introduction to Radiation Protection (5th edition), London: Hodder Arnold.

Matiullah, A., Ur-Rehman, Sh., Ur-Rehman, A. and Faheem, M. (2004). "Measurement of Radioactivity in the Soil of Behawalpur Division, Pakistan", Radiation Protection Dosimetry 112 (3): 443-447.

Mensah, M. A., Koranteng, K. A., Bortey, A. and Yeboah, D. A. (2001). The state of world fisheries from a fishworker perspective: the Ghanaian situation. International Collective in Support of Fishworkers, Chennai, India.

Ministry of Fisheries, (2006). Ministry of Fisheries 2005 annual report. MoFI, Accra, Ghana.

National Council on Radiation Protection and Measurements. (1975). "Natural Background Radiation in the United States", NCRP Report No.45. NCRP, Washington, D.C.

Neary, G. J. (1940). The b-Ray Spectrum of Radium E. Proc. Roy. Soc. London. 175A: 71.

Noz, M. E. and Maguire Jr., G. Q. (2007). Radiation Protection in the Health Sciences, London: World Scientific Publishing Co. Pte. Ltd.

Ntiamoa-Baidu, Y. (1995). Indigenous vs. introduced strategies: the case of protected area systems in Ghana. Issues in African Biodiversity, No. 1. Washington, D.C.: Biodiversity Support Program.

Nuclear Technology Education Consortium. Radioactive Decay. (2009). [cited 2013 27th of May]; Available from: http://www.ntec.ac.uk/Phys/pdfs/8-Radioactive%20Decay.pdf.

Oliveira, L., Antunes, A.M. and Bueno, M.I. (2010). Direct Chromium Speciation using X-ray Spectrometry and Chemometrics, X-ray Spectrometry, 39: 279-284.

Osenbrueck, K., Bretzler, A., Stadler, S., Ehser, A., Ruprecht, J.S., and Gloaguen, R. (2013). Groundwater flow pattern and water-rock interaction in the Ethiopian Rift Valley, Technical report of the Water & Earth System Science Research Centre, Univ. Tuebingen, Germany.

Othman, I. and Yassine T. (1995). Natural radioactivity in the Syrian environment. Science of the Total Environment, 1995. 170(1-2): 119-124.

Paschoa, A.S. (2000). More than forty years of studies of natural radio activity in Brazil. Technology 7: 193–212.

Pettijohn, F. J., Potter, P. E., & Siever, R. (1987). Sand and Sandstone. New York: Springer-Verlag

Pizarro, P., Rodriguez, S.T., Notario, N.P. and Gonzalez, J.M. (2008). Usefulness of chemometrics to classify pottery sherds belonging to the south east of USA, Paper presentation at the 2nd Ed of the Mediterranean meeting on Multivariate Analysis and Chemometry applied to Environmental and Cultural Heritage, Venstotene Island, Italy.

Quindos, L. S., Fernandez, P.I., Soto, J., Rodeanas, C., Gomez, J. (1994). Natural radioactivity in Spanish soils. Health Phys. 66: 194-200.

Radhakrishna A. P., Somashekarappa H. M., Narayana Y., Siddappa K. A. (1993). new natural background radiation area on the southwest coast of India. Health Phys. 65(4): 390–395.

Ramli, A.T. (1997). "Environmental Terrestrial Gamma Radiation Dose and its Relationship with Soil Type and Underlying Geological Formations in Pontian District, Malaysia", Applied Radiation and Isotopes 48 (3): 407-412.

Revil, A. and Glover, P. W. J. (1997). Theory of ionic-surface electrical conduction in porous media. *Physical Review B*, 55: 1757–1773.

Reyment, R. A. and Savazzi, E. (1999). *Aspects of Multivariate Statistical Analysis in Geology*. Elsevier Science B.V, Amsterdam.

Rutherford, E. (1911). The Scattering of Alpha and Beta Particles by Matter and the Structure of the Atom, University of Manchester. Philos. Mag. 6 (21).

Saad, H. R., Al-Azmi, D. (2002). Radioactivity concentrations in sediments and their correlation to the coastal structure in Kuwait. Applied Radiation and Isotopes, 56(6): 991-997.

Sakanoue, M. (1994). 'Determination of Very Low Levels of Radioactivity', International Union of Pure and Applied Chemistry, vol. 66, no. 12: 2537-2586

Saueia, C.H.R. and Mazzilli, B.P. (2006). "Distribution of Natural Radionuclides in the Production and Use of Phosphate Fertilizers in Brazil", Journal of Environmental Radioactivity 89: 229-239.

Sheppard, S.C. and Sheppard, M.I. (1988). Modeling estimates of the effect of acid rain on background radiation dose Environmental Health Perspectives, 78: 197–20

Singh S., Rani A., Mahajan R. K. (2005). ^{226}Ra, ^{232}Th and ^{40}K analysis in soil samples from some areas of Punjab and Himachal Pradesh, India using gamma ray spectrometry. Radiat. Meas 39: 431–439.

Sohrabi, M. M., BeitoUahi, M. M., Lasemi, Y. and Amin Sobhani, E. (1996). Origin of a new high level natural radiation area in hot spring region of Mahallat, Central Iran. in Proceedings of 4th International Conference on High Levels of Natural Radiation,. Beijing, China, 21-25, October.

Spalding, R. F. and Sacket, W. M. (1972). 'Uranium in Runoff from the Gulf of Mexico Distribution Province: Anomalous Concentration', Science, vol. 175: 629-631.

Swan, A. R. H. and Sandilands, M. (1995). *Introduction to Geological Data Analysis*.
Blackwell Science Ltd.

Tanaskovic, I., Golobocanin D. and Miljevic, N. (2012). Multivariate statistical analysis of hydrochemical and radiological data of Serbian spa waters Journal of Geochemical Exploration, 112: 226–234

Taskin, H.M., Karavus, P., Ay, A., Touzogh, S., Hindiroglu and Karaham, G. (2009). Radionuclide concentration in soil and lifetime cancer risk due to gamma radioactivity in Kirklareli, Turkey'. Journal of Environmental Radioactivity, Vol.100, pp.49-53.

Theodorsson, P. (1996). Measurement of Weak Radioactivity, London, World Scientific, ISBN: 978-981-02-2315-1.

TRACERCO, (2007). Module 14: Naturally Occurring Radioactive Material in Oil Production, Radiological Safety Course, 1-11.

Turner, J.E. (2007). Atoms, Radiation, and Radiation Protection (3rd edition), Weinheim: Wiley-VCH.

Tweneboah, E. (2001). Impacts of tourism on the coastal zone of Ghana: a comparative study of Ada and Elmina. MPhil Thesis. University of Ghana, Legon.

Tzortzis, M., Tsertos, H., Christofides, S., Christodoulides, G. (2003). Gamma-ray measurements of naturally occurring radioactive samples from Cyprus characteristic geological rocks. Radiation Measurements 37, 221–229.

Tzotzis, M., Svoukis, E. and Tsertos, H. (2004). "A Comprehensive Study of Natural Gamma Radioactivity Levels and Associated Dose Rates from Surface Soils in Cyprus", Radiation Protection Dosimetry 109 (3): 217-224.

United Nations Scientific Committee on the Effects of Atomic Radiation. (1982). Report to the General Assembly, with annexes. United Nations sales publication E.82.IX.8. United Nations, New York.

United Nations Scientific Committee on the Effects of Atomic Radiation. (1993). Report to the General Assembly, with scientific annexes. United Nations sales publication E.94.IX.2. United Nations, New York.

United Nations Scientific Committee on the Effects of Atomic Radiation. (2008). "Sources and Effects of Ionizing Radiation", UNSCEAR 2006 Report Vol.1 to the General Assembly, with scientific annexes, United Nations Sales Publication, United Nations, New York.

UNSCEAR, (2000). Sources and effects of ionizing radiation. United Nations Scientific Committee on the Effects of Atomic Radiation, United Nations, New York.

Van der Stritch, E. and Kirchmann, R. (2001). Radioecology: Radioactivity & Ecosystems, Belgium, Fortemps.

Voncina, E., Voncina, D.B., Mirkovic, N. and Norvic, M. (2007), Chemometric Characterization of the Quality of Ground Waters from Different Wells in Slovenia, Acta Chim. Slov. 54: 119-125.

Wackernagel, H. (2003). *Multivariate Geostatistics - An Introduction with Applications*. Third Edition, Springer-Verlag Berlin Heidelberg, Berlin.